Published in final edited form as:
Acta Biomater. 2011 January ; 7(1): 31–56. doi:10.1016/j.actbio.2010.07.028.

Liquid-liquid two phase systems for the production of porous hydrogels and hydrogel microspheres for biomedical applications: A tutorial review

Donald L. Elbert
Department of Biomedical Engineering and Center for Materials Innovation, Washington University in St. Louis, Campus Box 1097, One Brookings Dr., St. Louis, MO 63130

Abstract

Macroporous hydrogels may have direct applications in regenerative medicine as scaffolds to support tissue formation. Hydrogel microspheres may be used as drug delivery vehicles or as building blocks to assemble modular scaffolds. A variety of techniques exist to produce macroporous hydrogels and hydrogel microspheres. A subset of these relies on liquid-liquid two phase systems. Within this subset, vastly different types of polymerization processes are found. In this review, the history, terminology and classification of liquid-liquid two phase polymerization and crosslinking are described. Instructive examples of hydrogel microsphere and macroporous scaffold formation by precipitation/dispersion, emulsion and suspension polymerizations are used to illustrate the nature of these processes. The role of the kinetics of phase separation in determining the morphology of scaffolds and microspheres is also delineated. Brief descriptions of miniemulsion, microemulsion polymerization and ionotropic gelation are also included.

Keywords

review; thermally induced phase separation; aqueous two phase systems; suspension polymerization; emulsion polymerization; dispersion polymerization; precipitation polymerization; microemulsion; miniemulsion; phase inversion; porogen; colloid; coacervate; coacervation; PEG; NIPAAm; HEMA; gelatin; LCST; coarsening; coalescence; Ostwald ripening; pinning; syneresis; microsyneresis; scaffold; tissue engineering; regenerative medicine

I. Introduction

Porous scaffolds are useful in tissue engineering to enhance nutrient or waste transport, to allow vascularization, or to promote rapid ingrowth of cells. The production of porous scaffolds generally relies on the use of two phase systems, with one phase consisting of the scaffold material and the other phase serving as a porogen. The porogen may be a gas, liquid or solid. While the use of solid or gaseous porogens is not absolutely incompatible with cell survival, this has proven to be so in the vast majority of systems. For cell transplantation, this requires that the cells must be introduced into the scaffold after formation of the pores, which may result in a non-uniform distribution of cells. At the other end of the spectrum, non-macroporous bulk

hydrogels may be readily formed in the presence of cells, but the lack of porosity may be a limitation. Liquid-liquid phase separated systems may bridge the gap between macroporous scaffolds formed apart from cells and non-macroporous hydrogels formed in the presence of cells.

Liquid-liquid phase separations present a number of opportunities to precisely engineer the structure of hydrogel scaffolds. A phase-separated solution may be directly crosslinked to form a porous scaffold ('top-down' scaffold assembly). Alternatively, hydrogel microparticles may be produced in a liquid-liquid two phase system and then assembled into scaffolds ('bottom-up' scaffold assembly). Manipulation of the thermodynamics and kinetics of phase separations leads to a wide variety of morphologies of the phase-separated domains, which greatly impacts the architecture of macroporous scaffolds, or the size and porosity of microspheres. This review will highlight how different types of heterogeneous polymerizations produce distinct classes of hydrogel biomaterials.

Several excellent reviews on related topics are available in the literature. Methods to form macroporous scaffolds from non-hydrogel materials have been previously reviewed [1–3]. Microparticle production by mechanical means (e.g. photolithography, micromolding, droplet generators and microfluidics) has been reviewed [4,5]. Methods to produce nanogels, which are particularly useful for drug delivery applications, have been recently reviewed [6,7]. Self-assembling molecules to produce biomimetic materials have been considered elsewhere [8]. Reviews are available concerning "microgels" that form prior to gelation of crosslinking systems [9,10]. Additionally, reviews on hydrogel microparticle synthesis by Saunders et al. are highly recommended [11,12].

Liquid-liquid two phase systems are currently being exploited in a wide variety of intriguing ways in the fields of biomaterials and tissue engineering. In this review, the focus will be on selected examples of that particularly highlight the historical development or the benefits and limitations of the different polymerization strategies. It is hoped that clarification of the history and nature of liquid-liquid two-phase microgel/scaffold production methods will ignite further innovations in the production of novel macroporous biomaterials.

II. Polymerization schemes for the production of microspheres, microcapsules and porous materials via liquid-liquid two phase systems

Background

Four major types of two-phase systems are used for the production of microspheres and microcapsules: *emulsion polymerization*, *suspension polymerization*, *dispersion polymerization* and *precipitation polymerization.* The definitions of each polymerization type have not been codified by IUPAC. However, several sources are in general agreement. Arshady produced excellent review articles that delineate the differences between these four types of polymerization [13,14]. The definitions largely recapitulate those of Barrett in the monograph, *Dispersion Polymerization in Organic Media* [13,14]. Arshady and Barrett in turn relied on the definitions of Schildknecht in the book he edited from 1956, *Polymer Processes* [15]. The characteristics of the different polymerization types are summarized in Table 1 for chain growth (e.g. free radical) polymerizations and in Table 2 for step growth (i.e. polycondensation or polyaddition) polymerizations.

Solution, suspension and emulsion polymerizations

Solution polymerization is a single phase (homogenous) polymerization in which all constituents (monomers, initiators, etc.) are soluble in the polymerization medium. Many hydrogels used for biomedical applications are produced by solution polymerization, yielding

relatively homogenous materials. Examples include the photopolymerization of PEG-diacrylate [16], addition reactions of PEG-vinylsulfone with dithiol peptides [17], and cycloadditions of PEG-azide with peptide alkynes [18]. Cell viability is minimally affected by these chemistries. Unfortunately, introduction of macroporosity in the presence of living cells is less straightforward.

Polymerizations may also be conducted in heterogeneous, two phase or multiphase systems, with a monomer-rich phase suspended in a solvent-rich phase. The solvent-rich phase is typically called the continuous phase, since its volume is usually large compared to the monomer-rich phase. It remains topologically connected (percolated) throughout the volume. If the solvent-rich phase were present as the minority phase, a porous material would be directly produced upon polymerization of the percolated monomer-rich phase, with the pores formed by the solvent-rich phase. In the discussion below, it will be assumed that the monomer-rich phase exists as discrete droplets and the solvent-rich phase is the continuous phase.

Suspension polymerization is also called pearl, bead or granular polymerization [15]. In suspension polymerization, the monomer is 'insoluble' in the continuous phase, but in practice may have slight solubility (e.g. styrene in water) [15]. In suspension polymerization, initiation occurs within the monomer-rich droplets and with greater than one radical per droplet at any time [19]. The presence of multiple radicals per droplet results in termination kinetics that are similar to those observed in solution polymerization. Essentially, a solution polymerization occurs in each suspended monomer-rich droplet, although with better heat transfer due to the large total surface area.

Emulsion polymerization is also characterized by poor solubility of the monomer in the continuous phase, but with initiation occurring outside of the monomer droplets [15]. The initiator causes chain growth of the monomer dissolved in the majority phase or monomer contained in micelles if surfactants are present [15]. Large monomer droplets provide a source of monomer for the reaction, but polymerization does not occur within the monomer droplets. The relatively small surface area of the monomer droplets and the short lifetime of the radicals ensure that initiation occurs within the continuous phase or within micelles. As such, the size of particles produced does not depend on the dimensions of the monomer-rich droplets. The size of the monomer-rich droplets depends on the stirring rate, but stirring rate does not affect the size of the product. Since initiation in emulsion polymerization occurs apart from the large monomer droplets, the sizes of formed microparticles are dictated primarily by the number of polymerization loci generated outside the monomer droplets [19]. The size of formed microparticles is typically quite small, in the range of 100 nm, and often with low polydispersity in size [20]. To produce larger microspheres by emulsion polymerization, sub-micron microspheres formed by emulsion polymerization may be 'seeded', i.e. swollen in monomer, and polymerized a second time [21]. An emulsion/seeded polymerization process was used on the space shuttle to produce micron-sized polystyrene microspheres for use as calibration standards, which was the first commercial product made in space [22].

Distinguishing suspension polymerizations from emulsion polymerizations

Suspension polymerization may be distinguished from emulsion polymerization at first glance by the size of the particles formed. The monomer droplets that are polymerized in a suspension polymerization are typically much larger than 10 μm in diameter [20]. The size of the monomer droplets is determined by two major factors, the rate at which droplets are broken up by the input of mechanical energy (e.g. stirring rate) and the rate at which monomer droplets grow in size by merging with other droplets (coalescence) [23]. In a suspension polymerization, the large particles that form tend to aggregate and settle out, while a stable latex of particles may result from an emulsion polymerization [20].

Simplistically, suspension polymerization and emulsion polymerization may also be distinguished by the location of the initiator. The initiator and monomer are in the same phase in suspension polymerizations, while they are in separate phases in emulsion polymerization. More rigorously, the distinction relies on the kinetics of polymerization as delineated by Smith and Ewart in 1948 [24]. The rate of polymerization and the degree of polymerization of the product are influenced by the number of radicals per droplet. In suspension polymerizations, the number of radicals per droplet is typically much larger than one, with molecular weights limited by termination between macroradicals (Smith and Ewart case III). In an ideal emulsion polymerization, the number of free radicals per polymerization locus is one half. Termination of polymerization occurs rapidly when a second radical enters the polymerization locus, but otherwise either zero or one radical exist per polymerization locus. The rate is maximal when half of the loci contain no radical and half contain one radical. Thus, in the ideal case, a single free radical in a polymerization locus reacts with monomer unhindered, resulting in high molecular weights and rapid rates of polymerization (Smith and Ewart case II). Slower polymerizations result if the average number of radicals per polymerization locus is much less than one (Smith and Ewart case I).

“Emulsion polymerization” is a misnomer when applied to step growth (polycondensation or polyaddition) reactions (see Table 2). If the two condensing species are in different phases, the reaction is an interfacial polymerization. If the condensing species are in the same phase, the reaction is a suspension polymerization [14]. Smith & Ewalt kinetics are not relevant to step growth polymerizations.

Microemulsion/microsuspension/miniemulsion polymerizations

Thermodynamically unstable emulsions (i.e. ‘macroemulsions’) are used in conventional emulsion polymerizations and suspension polymerizations, both of which take place in the presence of large monomer droplets. With sufficient concentrations of emulsifier, thermodynamically stable emulsions (‘microemulsions’) may result. Microemulsions require surfactant concentrations much higher than the critical micelle concentration. Large monomer droplets are not present in microemulsions, as sufficient stabilizer exists such that monomer is present either within micelles or dissolved in the continuous phase [20]. The large surface area of the micelles results in efficient capture of radicals even if the initiator is in the continuous phase. This may result in kinetics that resemble suspension polymerization. If the initiator is in the monomer-rich phase, the size of the micelles may be so small that the average number of radicals is less than one. Thus, ‘microemulsion’ polymerization may have kinetics characteristic of a suspension polymerization, and ‘microsuspension’ polymerization may have kinetics characteristic of emulsion polymerization. It has been proposed that if either of the criteria (initiator location or kinetics) point to an emulsion polymerization, it should be characterized as a microemulsion polymerization [20]. Difficulty results when the polymerization kinetics are not characterized. Absent knowledge of the kinetics, the more general term ‘water-in-oil’ or ‘heterogeneous’ polymerization has been suggested but rarely applied [20].

An intermediate case exists when thermodynamically unstable but kinetically stable monomer droplets are generated. These are called ‘miniemulsions’ and require much less surfactant than microemulsions. Miniemulsions are produced by inputting large amounts of mechanical energy (e.g. sonication) resulting in submicron domains with relatively narrow size distributions [20]. Miniemulsion polymerizations take place within the small monomer droplets because of their large total surface area. Even if the initiator is in the continuous phase, capture of radicals by the monomer droplets is efficient and thus initiation occurs within droplets. The polymerization kinetics may approach those of a suspension polymerization regardless of the initial location of the initiator. Ideally, each monomer droplet will become a particle, typical

of suspension polymerization. However, some monomer droplets do not polymerize but contribute monomer to the growing particles. Thus, formed particles tend to be larger than the droplets [25].

While microemulsion polymerizations may occur even if the monomer and initiator are in the same phase, this is not true with macroemulsions. Suspension polymerization is the correct term in that case. This is because the average number of radicals per polymerization locus is almost certainly greater than one for these large phase separated domains. The size of the produced particles is an indication of the type of polymerization. Microemulsion polymerizations yield ≈ 100 nm particles, microsuspension polymerizations yields 1–10 μm particles, while suspension polymerizations yields particles typically much greater than 10 μm [20]. Confusion also results from the fact that suspension polymerizations and emulsion polymerizations both occur in macroemulsions [20]. Said another way, suspension polymerizations occurs in (macro)emulsions, but are not emulsion polymerizations.

“Inverse” systems

If the continuous phase is a water-immiscible solvent, then ‘inverse’ is often added to the classification (“direct” = oil-in-water polymerization, “inverse” = water-in-oil polymerization). Typically, the distinction between ‘direct’ and ‘inverse’ systems is clear from the context and is sometimes omitted. Great difficulties are encountered in classifying free-radical polymerizations in inverse systems compared to direct systems [26]. It is believed that partial solubility of the initiator in the aqueous phase or termination of polymerization by reaction of the radical with the emulsifier hinder true inverse emulsion polymerizations. In direct emulsion polymerization, the use of a charged initiator in the aqueous phase ensures extremely low solubility of the initiator in the organic/monomer phase. For inverse emulsion polymerizations, although the monomer may be predominantly dissolved in the organic phase, the initiator may have some limited solubility in the aqueous phase, particularly when large amounts of monomer are dissolved in the aqueous phase. This may result in kinetics that resemble an inverse suspension polymerization. Similar to direct microemulsions, the physical location of the initiator in an inverse microemulsion does not determine the kinetics of crosslinking. The term ‘inverse microemulsion’ is used if either the initiator location or the kinetics point to an emulsion polymerization [27].

Precipitation and dispersion polymerizations

Precipitation polymerization exploits differences in the solubility of monomer and polymer to produce microparticles. Larger polymer chains have lower solubility than smaller ones [28]. Above a specific molecular weight, phase separation may be favored. Precipitation polymerization initially begins as solution polymerizations in a single phase, homogenous system. Shortly after the start of the polymerization, a relatively high concentration of polymer chains is present, favoring phase separation by nucleation. Later in the polymerization, the concentration of polymer chains is low and existing particles capture the chains before nucleation of new particles can occur [29]. Thus, nucleation of particles occurs only for a brief period of time shortly after the start of the reaction. This often results in a narrow size distribution of particles. In a precipitation polymerization, surfactants are not included, so particle coarsening by coalescence is prevalent, leading in many cases to the formation of irregularly shaped particles with larger size distributions [30].

If surfactants or other stabilizers are used to prevent coalescence of particles, the precipitation polymerization is then called a *dispersion polymerization* [13,30]. Dispersion polymerizations originally referred to the polymerization of vinyl acetate in water in the presence of high concentrations of water soluble polymer [15]. However, vinyl acetate is only sparingly soluble in water, so this was either an emulsion or suspension polymerization, and not a type of

precipitation polymerization. Later, Barrett used dispersion polymerization to describe a precipitation polymerization in organic solvent in the presence of large amounts of stabilizer to prevent coalescence of particles [30]. Many monomers of commercial interest are soluble in organic solvents, favoring the use of precipitation or dispersion polymerization in organic media. Dispersion polymerization now refers simply to a stabilized precipitation polymerization. Some authors prefer to use precipitation polymerization even when stabilizers are used and when spherical, nearly monodisperse particles are produced. The terms will be used essentially interchangeably herein, with preference given to precipitation polymerization.

Definitions and conventions

Originally, *microgel* was defined by IUPAC as a "network of microscopic dimensions" [31]. In 2007, IUPAC changed the definition to a: "Particle of gel of any shape with an equivalent diameter of approximately 0.1 to 100 μm" [32]. A *nanogel* was also then defined as a: "Particle of gel of any shape with an equivalent diameter of approximately 1 to 100 nm". Microgel has also been used since 1949 to describe the highly crosslinked, high molecular weight polymer molecules that form during typical crosslinking reactions prior to gelation [33]. Such species are not predicted by the Flory-Stockmayer gelation theory [34,35], but are found experimentally, particularly in solution polymerizations conducted at low concentrations of monomer, which favors intramolecular crosslinking [33]. The sizes of such 'microgels' are typically hundreds of thousands or millions of Daltons and thus are submicron in diameter [10]. Microgels are typically only a small percentage of the mass of the polymerizing medium but are readily detected by light scattering. A broad range of molecular weights is present, including large amounts of unreacted monomer. The polydispersity of the mixture is much higher than the typical size distribution of 'microgels' produced by suspension, emulsion, precipitation or dispersion polymerization, micromolding, droplet generators, microfludics, etc.

Definitions of the pore sizes of materials have also evolved over time. IUPAC defined 'macroporous polymers' as having pore diameters between 50 nm - 1 μm, while 'mesoporous polymers' have pore diameters from 2 – 50 nm [36]. According to definitions proposed by Peppas and Langer and in common use in the biomaterials field, 'microporous' membranes have pore diameters between 10 – 50 nm and 'macroporous' membranes have pore diameters in the range of 50 nm – 1 μm. 'Non-porous' membranes have pores at the molecular level, e.g. between swollen macromolecular chains [37]. Consistent with these definitions, materials with pore diameters larger than 1 μm have been termed 'superporous' [38]. Given the trends of definitions in numerous fields (e.g. see nanogel and microgel above), it is proposed that 'nanoporous' be used for pore diameters up to 100 nm, 'microporous' for pore diameters between 100 nm and 1 μm, and 'macroporous' for pore diameters larger than 1 μm. This convention will be used herein.

The mean sizes of water-swollen nanogels, microgels and pores in macroporous scaffolds may be challenging to measure. Transmission electron microscopy and scanning electron microscopy are typically performed on dried samples, which may not reflect the swollen state of a hydrogel. In particular, porosity may be observed in non-macroporous hydrogels upon drying. The collapse of polymer chains during drying may result in the development of structures that are not present in the wet state. Including a non-macroporous hydrogel as a control is advisable when characterizing porosity in the dry state. It is also advisable to supplement studies in the dry state (electron microscopy, mercury intrusion porosimetry, etc.) with scanning confocal microscopy in the swollen state. Dynamic light scattering (DLS) is also useful to obtain not only an average hydrodynamic radius of microparticles but also a size distribution. However, the mean size obtained is a *z*-average, which is highly skewed towards large particles [39]. Additionally, obtaining size distributions from DLS requires solution of

an inverse problem that must make some assumptions about the nature of the underlying particle size distribution, which may not be accurate for a given sample [40]. For broad size distributions, fractionation, e.g. by gel permeation chromatography, is required to obtain reliable light scattering measurements.

Thermodynamics of phase separations

Phase separation of a polymer may occur due to changes in polymer molecular weight, solvent composition or temperature. Phase separation occurs when the composition dependence of the free energy of mixing (ΔF_{mix}), has at least two minima (see Figure 1A). For polymer blends, the free energy of mixing per monomer is:

$$\Delta F_{mix}=kT\left[\frac{\phi}{N_A}ln\,\phi+\frac{1-\phi}{N_B}ln(1-\phi)+\chi\phi(1-\phi)\right] \quad [1]$$

where k is Boltzman's constant, T is temperature, φ is the volume fraction of polymer A, χ is the Flory interaction parameter, N_A is the degree of polymerization of polymer A, and N_B is the degree of polymerization of polymer B. For polymer A dissolved in a solvent B, N_B is equal to 1. For further discussion, excellent introductory texts on the topic are available [41, 42].

Two phases may coexist at compositions that have the same chemical potential ($\partial\Delta F_{mix}/\partial\,\varphi$) and minimize the net free energy of mixing. These compositions define the binodal points at a particular temperature/solvent combination. With changes in temperature or solvent, the composition dependence of ΔF_{mix} changes due to changes in the Flory interaction parameter, resulting in new binodal points (χ-induced phase separation). Given multiple sets of binodal points, binodal lines may be drawn that not only reveal the composition of incipient phase separation, but also display the composition of the two phases. Due to the scattering of light during phase separation, the binodal is also called the *cloud point*. At compositions between the binodal points where $\partial^2\Delta F_{mix}/\partial\,\varphi^2 < 0$, the solution is unstable and spontaneously phase separates by *spinodal decomposition*. The inflection points, where $\partial^2\Delta F_{mix}/\partial\,\varphi^2 = 0$, are the spinodal points. Connected spinodal points form a spinodal line. At solution compositions between the two binodal points, but where $\partial^2\Delta F_{mix}/\partial\,\varphi^2 > 0$, the solution is metastable. Thermal fluctuations in composition are suppressed and phase separation occurs only by nucleation and growth.

At a critical value of the Flory interaction parameter, which is a function of temperature, the binodal and spinodal points collapse to a single point. If χ decreases with increasing temperature, the temperature of the critical point defines an upper critical solution temperature (UCST). Above this temperature, the polymer and solvent are stable at all compositions. If χ increases with increasing temperature, the temperature of the critical point defines a lower critical solution temperature (LCST) [42]. Note that at off critical compositions, the polymer solution may be outside the binodal points and thus stable even though beyond the critical temperature. Equation [1] also shows that increases in the degree of polymerization of the polymer, N_A, will affect the binodal and spinodal points (reaction-induced phase separation [43]) [28].

Water soluble polymers exhibit LCST behavior in water, for example poly(N-isopropylacrylamide) (poly(NIPAAm); LCST ≈ 31°C) [44] and poly(ethylene glycol) (PEG; LCST ≈ 95°C) [45]. Using PEG as an example, the nature of LCST behavior can be further explored. The origin of LCST behavior of PEG in water is the destabilization of hydrogen bonding at elevated temperatures that disrupts the hydration shell surrounding the polymers [46]. A phase diagram for PEG in water is shown in Figure 1B [47]. PEG of low molecular

weight has a UCST greater than its LCST, leading to closed loop phase diagrams [48]. As the molecular weight of PEG increases, the LCST decreases. Thus, a precipitation polymerization of PEG macromonomers could be conducted in pure water at temperatures between about 100–150°C. Salts, particularly “water-structure breaking” salts of the Hofmeister series (kosmotropes), can greatly decrease its LCST (Figure 1C) [49,50]. Increased pressure also lowers the LCST of PEG (Figure 1D) [51,52]. Aqueous mixtures of water-soluble polymers may also undergo phase separations, such as dextran and PEG in water [53]. The phase behavior of other water soluble polymers is similar and has been catalogued in great detail [54].

Phase separation may occur without mixing by solvent evaporation in thin films or by a simple change in temperature (a *thermally induced phase separation*; Figure 2). The spinodal points are often quickly surpassed, ensuring that phase separation occurs by spinodal decomposition instead of nucleation and growth. In the early stages of spinodal decomposition, phase domains exist as rapidly growing concentration fluctuations on molecular length scales. The concentration fluctuations rapidly evolve into a bicontinuous (doubly percolated) network if the volume fractions of the two formed phases are similar. Due to surface tension, the characteristic size of the percolated domains grows as the liquid phases flow to become more spherical [55]. During this hydrodynamic process, the average size of the phase domains grows linearly with time. Once spherical domains form, the domains are physically separated and grow in size by mass transfer rather than by fluid flow, causing a change in the growth law that defines the *percolation-to-cluster transition* (Figure 3) [56]. ‘Coarsening’ or ‘ripening’ of the spherical domains occurs by coalescence (direct merger of droplets) or Ostwald ripening (diffusion of molecules from smaller, less stable droplets to larger, more stable droplets). In both coalescence and Ostwald ripening, average domain sizes grow with the cube root of time [56]. Due to the slower growth during the latter phase, the mean size of the domains is said to be ‘pinned’ at the percolation-to-cluster transition [57]. The sizes of the domains are not truly pinned to a certain value, but simply grow at a much slower rate [56]. The evolution of phase morphology towards the equilibrium state may be observed by light and neutron scattering, or directly by scanning confocal microscopy (Figure 4A) [57,58]. At long times, the two phases generally form two distinct macroscopic layers due to density differences between the phases. The coarsening process may be ‘pinned’ by vitrification, crystallization or gelation [57]. The morphology of the pinned phase domains will influence the mechanical properties of a material [59].

Cahn and Hilliard developed a model of phase separation by spinodal decomposition and coarsening by Ostwald ripening (Figure 4B) [60, 61]. This model is particularly suited for phase separations in solids or viscous solutions, e.g. in polymer/polymer blends, in which diffusion of phase domains is hindered, slowing coalescence. In less viscous solutions, coalescence may dominate due to the ability of the phase separated domains to encounter each other by diffusion [56]. With mechanical stirring, droplets will encounter each other frequently and the kinetics of the phase separation process will be similar to those that govern droplet size in a stirred suspension polymerization [23].

Gelation is itself a form of phase separation. The free energy of mixing as calculated by equation [1] (with the degree of polymerization of the gel, N_A, equal to infinity) is added to the elastic free energy change due to chain stretching within the swollen network. The elastic free energy is a function of the crosslink density, ν and the volume fraction of polymer, φ. The phase outside the gel is assumed to have no polymer and the chemical potential with respect to the polymer is thus equal to zero. The amount of solvent in the gel, and thus the equilibrium swelling of the gel, exist where the chemical potential in the gel phase is also zero (Figure 5) [62]. If more solvent is present during crosslinking than the equilibrium amount in the gel, the solvent will be exuded from the gel (*syneresis*, specifically, ν-induced syneresis). If further crosslinking traps solvent in the gel, solvent-rich pores may form within the gel (*microsyneresis*) [63]. Dusek

also described a second type of syneresis, χ-induced syneresis, where a change in the Flory interaction parameter drives phase separation [63, 64]. Syneresis occurs within the gel phase, where N_A is infinity, so it must be induced by changes in ν or χ. However, under conditions that promote precipitation polymerization, the formation of polymer particles may introduce heterogeneity prior to gelation, resulting in porosity by a mechanism that differs from ν-induced or χ-induced microsyneresis.

Colloidal properties of phase separated systems

Proteins and polysaccharides dissolved in water undergo phase separation at certain temperatures and solvent compositions [65]. The nature of the phase separation of biomacromolecules is thermodynamically equivalent to those encountered with polymers. However, the study of the phase behavior of proteins and polysaccharides pre-dated the routine synthesis of polymers, and different terminology developed.

Colloids are defined by their size (1–1000 nm) [66]. Colloids must be stabilized in some manner to prevent aggregation. Two types of stabilization are common, electrostatic and steric. Electrostatic stabilization results from the presence of like charges on all of the colloidal particles, which causes repulsion due to overlap of the electric double layers that surround the particles. Steric stabilization relies on the presence of solvent-soluble polymers attached to the surface of the colloidal particles. Overlap of polymer chains upon close approach of two particles is unfavorable. In both steric and electrostatic stabilization, long range repulsion prevents the close contact required for aggregation by van der Waals forces. Electrostatic stabilization is ineffective in high salt solutions and in organic solvents with low dielectric constants, due to the decrease in thickness of the electric double layer to the point that shorter-range attractive forces may overcome electrostatic repulsion. Steric stabilization is required in these cases [67].

Phase separation of polymers, proteins or polysaccharides may lead to the formation of solid precipitates or flocs that retain extremely low amounts of solvent. However, if more solvent is retained in the polymer-rich phase, two liquid phases result. In the colloid literature, a liquid-liquid two-phase solution is a *coacervate* [65]. Phase separation to form liquid-liquid two phase systems also occurs following the interaction of oppositely charged macromolecules, such as gelatin and gum arabic or poly(lysine) and alginate. This is termed *complex coacervation*, contrasted with a one component *simple coacervate* [65]. The difference between coacervation and precipitation is simply the amount of solvent retained in the polymer-rich phase [68].

III. Instructive examples of liquid-liquid two phase systems for the production of microspheres and macroporous hydrogels

Precipitation polymerization for the formation of hydrogel scaffolds

Wichterle and Lim introduced hydrogels to the biomedical community in 1960 [69]. In the original manuscript in *Nature*, the authors state, “Gels based on glycolmethacrylates are also noteworthy for their transparency (in the case of polyglycolmonomethacrylate with a water content less than 30 percent and with the higher glycols at all concentrations)”. Glycolmonomethacrylate is now known as 2-hydroxylethylmethacrylate (HEMA), which is typically crosslinked with a small amount of ethylene glycol dimethacrylate. The ‘higher glycols’ referred to are oligoethylene glycols, which were produced by reacting ethylene oxide gas with methacrylic acid. The “transparent gels at all water contents” were thus formed from a mixture of poly(ethylene glycol)-monomethacrylate and poly(ethylene glycol)-dimethacrylate [70,71]. This is not to be confused with poly(ethylene glycol methacrylate) or polyglycolmonomethacrylate, which are simply poly(HEMA) [72]. Unlike PEG-based hydrogels, the poly(HEMA) hydrogels were cloudy at high water contents. This was due to

the propensity of poly(HEMA) to phase separate from water. Above a degree of polymerization of 30, the cloud point of HEMA in water is less than 40°C, while the monomer and smaller oligomers are completely miscible [73].

Non-macroporous poly(HEMA) materials are typically produced neat or in alcohols with only a small amount of water present. Polymerization of HEMA in 60–90 wt% water resulted in the formation of a porous hydrogel sponge (Figure 6A). As described by the authors, “The initially excellent solubility of the monomers in water decreases sharply with increasing conversion and phase separation takes place” [74]. The sponges consisted of what appeared to be aggregated microspheres, less than about 10 μm in diameter and with low size dispersity. This suggests a precipitation polymerization with aggregation and crosslinking of the formed particles. Wichterle and Lim originally described the result of the polymerization of HEMA in water as follows: “With a water content greater than corresponds to the equilibrium capacity of the gel, a porous structure will arise by coalescing of the water-phase droplets into interconnected channels” [69]. This implies that the authors believed the cloudiness was caused by ν-induced microsyneresis, which is a different mechanism from precipitation polymerization. Evidence that precipitation polymerization is the dominant mechanism is that poly(HEMA) microspheres may be formed if the HEMA concentration in water is decreased (described in detail in the next section). Thus, porosity of hydrogels may not always be readily explained in terms of microsyneresis.

Sponges formed in 50–60% water that were implanted in animals became surrounded by a fibrous capsule similar to non-macroporous HEMA hydrogels. Higher water content during polymerization produced pores large enough for the ingrowth of cells into the sponge. Increased porosity resulted in smaller fibrous capsules and better vascularization [75]. It was observed that the microarchitecture of materials (pore size), rather than surface chemistry, enhanced the integration of the material with the host’s vascular system [76]. Enhanced vascularization may promote survival of transplanted cells, enhance endothelialization of vascular grafts or reduce diffusion limitations of biosensors [77].

In 1983, macroporous HEMA membranes were used to form containers for the transplantation of pancreas tissue [78]. The goal was to enhance the transport of insulin while preventing ingrowth of leucocytes. As such, the membranes were not porous enough to vascularize, but were surrounded by a thin, vascularized fibrous capsule [79]. The enhanced transport properties of macroporous HEMA membranes led to their use in a glucose sensor that also released insulin [80]. Spongy HEMA hydrogels have been used for breast augmentation and as replacements for articular cartilage [81,82]. However, the propensity of HEMA hydrogels to calcify and in some cases cause tumors has been noted [83,84]. Furthermore, calcification may be enhanced by macroporosity [85].

Interest in macroporous HEMA hydrogels was later revived due to their potential to promote tissue ingrowth. Chirila and colleagues produced a homogenous poly(HEMA) hydrogel surrounded by a macroporous poly(HEMA) skirt, which has been used for clinical corneal replacement (Figure 6B) [86]. Lowman and colleagues used HEMA to form porous sponges, finding that sonication aided in developing uniform pores. The authors speculated that non-uniformity may have resulted from the formation of nitrogen gas bubbles as the initiator, 2,2-azobis(2-azobis(2-methyl-proprionitrile) (AIBN), decomposed [87]. Phase separation was tolerant to small amounts of poly(ethylene glycol) monomethylether monomethacrylate mol. wt. 200 included in the reaction mixture. The grafted PEG chains enhanced the interconnectivity of the pores, perhaps by delaying phase separation. Greater pore interconnectivity allowed endothelial cells to enter the sponges and form tubules [88]. Such endothelial tubules are significant because rapid vascularization of scaffolds may require the presence of preformed tubules that join to the host’s vasculature [89].

Shoichet and colleagues polymerized HEMA and methyl methacrylate in water to make macroporous nerve guidance conduits. The polymerization reaction began as a homogenous solution that was placed in a sealed tube and spun at 2500 rpm on a drill. The denser polymer migrated to the outer edge of the tube, forming a hollow fiber membrane. Polymerization of pure HEMA in water resulted in highly porous membranes. At higher water contents, a beaded morphology was observed, consistent with the coalescence of microparticles formed by precipitation polymerization (Figure 7A). At slightly lower water contents, a microporous membrane formed. The water concentration was above the equilibrium water concentration of the gels, so the micropores likely resulted from ν-induced microsyneresis (Figure 7B). Addition of methyl methacrylate to the reaction resulted in a highly porous inner layer and a more continuous outer layer with large, unconnected pores (Figure 7C). The inner layer was likely the result of a precipitation polymerization. The outer layer may have been enriched in methyl methacrylate and phase separated early in the reaction. The phase separation reached an advanced stage before gelation, producing a nearly homogenous network. The large pores in the outer layer were most likely the result of ν-induced microsyneresis [90–92]. These materials clearly illustrate that subtle changes in polymerization conditions may lead to vastly different modes of polymerization and pore formation.

Other water soluble polymers also undergo phase separation in water and this may be exploited to produce macroporous hydrogels. Poly(vinylmethylether), which has a cloud point of around 37°C, was crosslinked by gamma radiation from a ^{60}Co source, resulting in a porous gel. The hydrogels exhibited rapid swelling and deswelling near the LCST of poly(vinylmethylether), attributed to the porous nature of the hydrogel. The hydrogel may have been porous due to a rise in temperature during crosslinking leading to phase separation of the polymer [93]. However, radiation crosslinking may generate hydrogen gas, so the role of gas bubbles in generating porosity was difficult to discern [94]. To avoid radiation crosslinking, the more reactive acrylamide group on N-isopropylacrylamide (NIPAAm) was used in a precipitation polymerization with a heat-initiated free radical polymerization. NIPAAm is water soluble at high temperatures, while poly(NIPAAm has an LCST of about 31°C [44]. NIPAAm thus forms macroporous hydrogels if polymerized at elevated temperatures [95]. Hoffman and colleagues further increased the porosity of poly(NIPAAm) hydrogels by adding hydroxypropyl cellulose to the monomer solution, which has an LCST of about 42°C. The hydroxypropyl cellulose precipitated at the polymerization temperature of 50°C along with the newly formed poly (NIPAAm). The cellulose particles were then extracted in water following polymerization, producing a highly porous scaffold with rapid swelling and deswelling kinetics [96,97]. Gotoh et al. compared the swelling and strength of poly(N,N'-diethylacrylamide) hydrogels and poly (NIPAAm) hydrogels, both crosslinked with N-N'-methylenebis(acrylamide) (BIS). Both polymers showed LCST behavior and both types of hydrogels formed porous 'aggregated bead' structures at temperatures above the LCST of the polymer. However, the poly(N,N'-diethylacrylamide) hydrogels did not form the porous structures unless formed well above the LCST, while poly(NIPAAm) hydrogels were porous even when polymerized at the LCST [98]. Such temperature sensitive gels undergo macrosyneresis as the temperature is raised above the LCST of the polymer, an example of χ-induced syneresis.

Shoichet and colleagues exploited the phase separation properties of PEG and dextran to produce macroporous scaffolds. Dextran-methacrylate that was crosslinked within a narrow range of PEG concentrations yielded architectures that by SEM appeared to be coalesced beads in the micron-size range (Figure 8A). Lower PEG concentrations produced non-macroporous dextran hydrogels, while higher PEG concentrations produced heterogeneous suspensions. The results suggested that the macromonomer (dextran-methacrylate) was soluble below a threshold concentration of PEG and precipitated only during the polymerization. Increasing the amount of dextran-methacrylate macromonomer resulted in structures that appeared to be continuous hydrogel containing large pores filled with beaded hydrogel (Figure 8B) [99]. The

continuous portion of the hydrogel may have resulted from a phase separation of the dextran-methacrylate macromonomer and PEG prior to gelation. The solutions were mixed, perhaps resulting in suspended PEG-rich droplets that became trapped in the hydrogel. The beaded structure that formed within the pores in Fig. 8B suggests a precipitation polymerization. Phase diagrams for PEG and dextran-methacrylate reveal that at the polymerization conditions shown in Figure 8B, the PEG-rich phase may contain up to about 7.5% dextran-methacrylate [100]. The dextran-methacrylate dissolved in the PEG-rich phase may have polymerized and then precipitated to yield the beaded structures within the large pores.

Righetti et al. found that poly(acrylamide) gels crosslinked with BIS undergo phase separation in the presence of non-crosslinkable water-soluble polymers, resulting in pore formation [101]. Acrylamide was completely soluble in PEG solutions, but poly(acrylamide) underwent phase separation during polymerization, even in the absence of the BIS crosslinker [102]. Scanning electron microscopy suggested that the poly(acrylamide) formed fibers around spherical pores (Figure 9A) [101,103]. As the PEG concentration increased, the sizes of the pores also increased. This may be explained by referring to the hypothetical ternary phase diagram in Figure 9B. Initially, the concentration of poly(acrylamide) is zero. During polymerization, the concentration of poly(acrylamide) increases until the binodal of the two phase region is reached. If the binodal is reached earlier in the crosslinking process, i.e. at a high PEG concentration, the phase-separated solution had more time to coarsen before the process is halted by gelation, resulting in larger pores [102]. Macroporous gels were also generated by crosslinking poly(acrylamide) in the presence of hydroxymethylcellulose or poly (vinyl pyrrolidone) [101]. Initially, the authors believed that crystallization of poly(acrylamide) chains caused defects in crosslinking of the network that resulted in pore formation [104]. Only later did light scattering reveal that phase separation by spinodal decomposition occurred, with coarsening over time that was halted by gelation [102]. Kwok et al. have catalogued the conditions for precipitation polymerization of poly(acrylamide) and other water soluble polymers in a variety of solvents [105–108]. More recent examples of precipitation polymerizations to produce macroporous gels have been reviewed [64].

Precipitation/dispersion polymerization for the formation of hydrogel microspheres

Early method development—While radiation crosslinking of HEMA in the presence of BIS usually resulted in the formation of a macroporous scaffold, discrete microspheres could also be produced by precipitation polymerization (Figure 10A). In 1976, Rembaum et al. used less than 5% w/w monomer to produce crosslinked HEMA microspheres (90% HEMA/10% BIS). Higher concentrations of monomer could be used if 0.4% PEG was included. Microspheres formed in the presence of PEG were more resistant to sodium chloride-induced aggregation, which suggested that the PEG became grafted to the microspheres. Bound PEG may sterically stabilize the growing particles, hindering coalescence and aggregation [109].

The LCST properties of poly(NIPAAm) may also be exploited to produce microspheres by precipitation/dispersion polymerization. In 1986, Pelton and Chibante published a method to produce monodisperse particles of NIPAAm or NIPAAm/acrylamide crosslinked with BIS (Figure 10B). Potassium persulfate or 2,2’-azobis(2-amidinopropane)·HCl were used as initiators to impart a negative or positive charge, respectively, at one terminus of the growing chain. Deionized water was the solvent and the polymerizations were performed at 60°C and higher. Lower temperatures did not result in microsphere formation. Concentrations of monomers above 2.5% resulted in the formation of precipitates. Increasing the concentration of acrylamide relative to NIPAAm also resulted in the formation of precipitates, although at very high ratios of acrylamide to NIPAAm, the formed polymer chains did not precipitate at all [110]. Formation of a monodisperse product thus occurred only over only a small range of experimental conditions. Kawaguchi et al. used this method to produce monodisperse poly

(NIPAAm) microspheres and demonstrated that protein adsorption was higher on the poly (NIPAAm) microspheres above the LCST than below. The microspheres deswelled thirteen fold as the temperature was raised above the LCST and the less swollen state promoted about a three-fold increase in protein adsorption [111]. Peppas and colleagues later demonstrated that polyethylene glycol-monomethacrylate could be co-polymerized with NIPAAm monomer to produce poly(NIPAAm-co-PEG) microspheres by dispersion polymerization [112].

Kawaguchi et al. adapted the Pelton and Chibante method to produce temperature sensitive microspheres with other acrylamide monomers - acryloyl pyrrolidine and acryloyl piperidine. Poly(acryloyl pyrrolidine) had an LCST of 50°C and poly(acryloyl piperidine) had an LCST of 5°C. Polymerization with BIS in water at 70°C produced about 1 μm diameter monodisperse microspheres. Adding up to 5% ethanol, a good solvent for the polymers, delayed precipitation and produced slightly larger particles. The formed particles could also be used as 'seeds' in subsequent polymerization, slightly increasing the particle size [113]. Attempts to produce microspheres with only acrylamide and BIS were undertaken by carrying out the polymerization in water/alcohol mixtures. The alcohols were needed as non-solvents for the poly(acrylamide), due to the high water-solubility of this polymer. Microspheres with low polydispersity in size were produced, but these aggregated into ≈ 100 μm clusters. Including only a fraction of a percent of methacyrlic acid prevented aggregation and produced ≈ 1 μm diameter monodisperse poly(acrylamide) microspheres (Figure 10C) [114].

A few examples follow of microspheres formed by precipitation polymerization that were used to produce macroporous materials, drug delivery vehicles and surface coatings.

Scaffold assembly from microspheres—Colloids of equal size pack into ordered structures (colloidal crystals) that are iridescent due to the nature of light scattering from the regularly spaced particles [115]. Asher and colleagues produced poly(NIPAAm-*co*-2-acrylamido-2-methyl-1-propanesulfonic acid) microgels based on the Pelton and Chibante protocol. The microgels self assembled into colloidal crystals that scattered light due to the ordered structure of the material [116]. The size of the poly(NIPAAm) microspheres produced by precipitation polymerization was controllable by the concentration of BIS in the reaction. Changes in microsphere size affected the light scattering of self-assembled scaffolds [117]. Lyon and colleagues demonstrated that poly(NIPAAm-co-acrylic acid) microgels assemble into iridescent colloidal crystals that persist for some period of time without chemical crosslinking [118,119]. If the scaffolds of poly(NIPAAm-co-acrylic acid) microgels were assembled in the presence of colloidal gold, exposure to a narrow beam of laser light caused contraction of the colloidal crystal within the beam, leading to the formation of a lens-like structure [120,121]. The unusual phase behavior of these non-crosslinked thermosensitive colloidal crystals has been reviewed [122].

Hu et al. produced crosslinked scaffolds from poly(NIPAAm) microspheres by precipitation polymerization (mischaracterized as an emulsion polymerization) [123]. The microspheres were crosslinked with epichlorohydrin or divinylsulfone to form scaffolds that exhibited opalescence (iridescence; Figure 11A) [124]. Similarly, copolymerization of NIPAAm with allylamine in a precipitation polymerization produced microspheres that could be crosslinked with glutaraldehyde in the presence of dextran, serving as a model for a drug delivery system [125]. The precipitation polymerization technique was also adapted to produce microspheres of 2-(2-methoxyethoxy)ethyl methacrylate and oligoethylene glycol-methacrylate, taking advantage of the temperature-sensitive properties of the first component [126]. A related patent application describes the non-covalent self assembly of microparticles of poly(HEMA) produced by precipitation polymerization [127]. Cai & Gupta demonstrated that packed poly (NIPAAm) microgels could be crosslinked into scaffolds by adding NIPAAm and BIS and initiating polymerization. The monomers may have reacted with residual acrylamide groups

in the microgels or may have simply diffused into the microgels to form an interpenetrating network [128].

Weitz and colleagues also assembled poly(NIPAAm) microspheres into three dimensional materials. Copolymerization of NIPAAm and allylamine by precipitation polymerization produced microgels. In the presence of poly(acrylic acid) and above the LCST of NIPAAm, the microgels aggregated and were crosslinked by glutaraldehyde. Due to the presence of pores resulting from packing defects, scaffolds assembled from microgels exhibited about two orders of magnitude more rapid swelling than bulk gels. The microgels were conjugated to antibodies to add bioactivity, or mixed with silica particles, polystyrene microspheres or magnetic nanoparticles to add different properties to the scaffolds [129,130]. The microgels segregated to silicone oil/water interfaces due to the hydrophilic amide and the hydrophobic isopropyl groups. Crosslinking of amine groups in the microgels resulted in stable shells of microgel, referred to as ‘colloidosomes’. Uniform sized colloidosomes were also produced using a microfluidics device [131].

Wu and Shen used dispersion polymerization of polyacrylamide to produce micron sized microspheres that could be crosslinked to form an injectable sealant. Some microspheres were copolymers of acrylamide with aminoethyl methacrylate, while others contained acetoacetoxyethyl methacrylate, which contains an ester that may be aminolysed. Upon mixing, the two types of microspheres reacted, forming a crosslinked gel within 90 seconds [132].

Kawaguchi and colleagues produced poly(NIPAAm) microgels by precipitation polymerization and used these to produce Janus particles. Janus particles have different chemistries on opposite halves of the particles. Carboxyl-containing poly(NIPAAm) microgels were used to stabilize an emulsion of hexadecane in water, with the microgels in essence serving as a surfactant. Activation of the carboxylic acids with a water-soluble carbodiimide and ethylenediamine promoted functionalization of the water-facing side of the microgels. The resulting microparticles were shown to stack into chains of microgels at pH 4 [133]. This suggests an ability to direct the self-assembly of microspheres into scaffolds with complex architectures.

Selected drug delivery applications—Thermally responsive microspheres have been used extensively for drug delivery applications and only a few examples will be described. Kiser et al. produced monodisperse microgels from methacrylic acid crosslinked with BIS by the precipitation polymerization methods of Kawaguchi. The anionic microgels were loaded with the cationic drug doxorubicin. The microspheres were deswelled in acidic solutions and coated with a phospholipid bilayer. Upon return to physiological pH, the microgels stayed at the dehydrated size until the lipid bilayer was broken by electroporation. The pH equilibrated rapidly after rupture of the membrane, the microgels swelled and the drug was released [134–136]. Positively charged, infrared absorbing gold nanorods have been attached to negatively charged poly(NIPAAm-co-acrylic acid) microgels, producing materials that underwent photothermally triggered swelling and drug release [137,138]. Hoare and Pelton added an acrylated phenylboronic acid to poly(NIPPAAm) microgels produced by precipitation polymerization. The microgels were loaded with insulin and binding of glucose to the phenylboronic acid resulted in gel swelling that promoted insulin release [139].

Surface coatings from microspheres—Griffith and colleagues used a dispersion polymerization of methyl methacrylate in 1:1 ethanol:water to produce microspheres non-covalently coated with a PEG/methyl methacrylate copolymer surfactant. The surfactant was of high molecular weight and water-insoluble, and thus bound strongly to poly(methyl methacrylate) microspheres. The microspheres were then spin coated onto substrates and

melted to form films. The films retained the PEG-containing stabilizer and thus had hydrophilic surfaces. The films resisted cell adhesion, unless a cell-adhesive RGD peptide was coupled to the stabilizer prior to the dispersion polymerization. The stabilizer itself could also be dissolved in ethanol/water and spin coated onto substrates, producing films that resisted non-specific cell adhesion. Microspheres containing RGD were embedded in continuous films of stabilizer that did not contain RGD, presenting cell adhesion peptide to cells at discrete locations [140].

Poly(NIPAAm-co-acrylic acid) microspheres were electrostatically coated on aminosilanated glass and assembled into polyelectrolyte multilayer structures with a polycation by Lyon and colleagues. The films were loaded with drug (doxorubicin or insulin) below the LCST, which was released rapidly by raising the temperature above the LCST to deswell the film [141, 142]. To reduce protein adsorption at physiological temperatures, PEG was added to the microgels. A two stage polymerization was used, with poly(NIPAAm) cores formed first and then ‘seeded’ with PEG macromonomer. However, protein adsorption to the microspheres was substantial unless high amounts of PEG were included in the core, without addition of a shell [143,144]. The PEG/NIPAAm microgels were covalently coupled to poly(ethylene terephthalate) (PET) substrates (Figure 11B). The PET was modified in an argon plasma to introduce groups that produce free radicals to initiate polymerization of acrylic acid. The poly (acrylic acid) on the surface was activated with ethyl-3-[3-dimethyl amino] propyl carbodiimide (EDC) and N-hydroxysuccinimide (NHS) and coupled to an amine-containing benzophenone photoinitiator. Microgels were deposited on the surface by spin coating and coupled to the surface by exposure to UV light. The microgels were detected on the surface by AFM and resisted cell adhesion [145]. Following implantation in mice, fewer leukocytes adhered to the microgel-coated materials compared to uncoated PET [146]. Additional surface coatings based on responsive microgels have been reviewed [147].

Suspension polymerization with organic continuous phase

Suspension polymerization was first described in a German patent from 1931 [15]. The main advantage of suspension polymerization is better heat transfer, important due to high heats of polymerization, and the direct formation of a granular product that can be easily processed [15]. An early example of inverse suspension polymerization to produce hydrogel microspheres was the polymerization of dextran to produce a product now known as Sephadex [148,149]. Aqueous solutions of dextran were suspended in toluene with poly(vinyl acetate) as a stabilizer and crosslinked with epichlorohydrin [150]. In another early study, dextran microspheres were produced by acrylating dextran and performing a free radical polymerization in water suspended in chloroform. Enzymes were trapped within the microspheres and retained about 50% of their activity. The enzymes were released in a controlled manner over a few months. The enzymes also demonstrated greater heat stability when trapped in the microspheres [151]. Since that time, water-in-oil suspension polymerizations have been so commonly practiced that the focus will be on a few biomaterials-related examples of the formation of poly(NIPAAm), poly(ethylene glycol), hyaluronic acid and gelatin microspheres. Alginate microsphere formation by suspension polymerization has recently been reviewed [152].

Although poly(NIPAAm) hydrogel microspheres are typically formed by precipitation polymerization, inverse suspension polymerization below the LCST is also possible. In 1985, Tanaka and colleagues found that polymerization of NIPAAm suspended in paraffin oil resulted in microspheres with diameters in the range 0.1–1.5 mm (note the large size compared to precipitation polymerization) [153]. Later, they also copolymerized NIPAAM and N-(acryloxy)succinimide, with hexane as the suspending medium, SPAN 20 as the emulsifier, and ammonium persulfate (APS) as the initiator. Swollen microspheres in the submicron range were found by dynamic light scattering after passage through a 5 μm filter. However, optical

microscopy revealed the presence of microspheres with diameters of up to 240 μm in diameter. This illustrates the high polydispersity in size found with suspension polymerizations, which the authors mischaracterized as an inverse emulsion polymerization [154]. In 1988, Park & Hoffman produced poly(NIPAAm-co-acrylamide) microspheres by inverse suspension polymerization at room temperature. The suspending medium was paraffin oil, Pluronic L-81 was the emulsifier, and APS was the initiator, producing microspheres 200–400 μm in diameter. The microspheres entrapped the enzyme β-galactosidase, which was found to be active below the LCST of poly(NIPAAm) but inactive above the LCST [155].

Peppas and colleagues produced microspheres that were 50% by weight poly(ethylene glycol) by inverse suspension polymerization. Monomethoxypoly(ethylene glycol) monomethacrylate 1000 was copolymerized with methacrylic acid in water that was suspended in silicone oil. Tetraethyleneglycol dimethacrylate was used as a crosslinker, AIBN was the initiator and poly (dimethylsiloxane-*b*-ethylene oxide) was the surfactant. The surfactant had little effect on mean microsphere size (about 25 μm) but did reduce the size distribution [156]. Although AIBN is soluble in organic solvents, the sizes of the microspheres suggested an inverse suspension polymerization rather than an emulsion polymerization, perhaps due to partial solubility of the AIBN in water.

Inverse suspension polymerization is also commonly used to produce PEG-based peptide synthesis resins [157,158]. Ulijn and colleagues started with these resins and synthesized peptides with balanced positive and negative charges at neutral pH. Under acidic conditions, the particles became positively charged and swelled. The swollen microspheres were incubated with protein solutions, trapping the proteins by returning to neutral pH. Upon enzymatic cleavage of the peptide with thermolysin, the particles again became charged, swelled, and released the loaded protein [159–161]. Degradable PEG-diacrylate has also been free-radical crosslinked after suspension in mineral oil. This produced PEG microspheres with average sizes in the range of ≈ 100–350 μm, which were used as porogens in poly(epsilon-caprolactone)-based scaffolds (Figure 12A) [162].

Hyaluronic acid has been crosslinked by inverse suspension polymerization to produce microspheres. Chen and colleagues reacted carboxyl groups on hyaluronan with adipic dihydrazide using EDC. The reacting solution was suspended in mineral oil with Span 80 as a stabilizer. The reaction was performed in the presence of plasmid DNA. Release of the DNA was triggered by incubation of the microspheres with hyaluronidase [163]. Jia et al. produced hyaluronic acid modified with aldehydes or amines. The modified hyaluronic acids were dissolved in water and homogenized in mineral oil using Span 80 as a stabilizer, producing microgels about 10 μm in diameter (Figure 12B). Microgels were then incubated with aldehyde and/or amine-modified hyaluronic acid to form a doubly crosslinked scaffold [164]. In another application of these hyaluronic acid microspheres, aldehyde groups in the microspheres were capped and the remaining amines were reacted with PEG-dialdehyde, which was then coupled to perlecan domain I modified with heparan sulfate. This enhanced binding of heparin-binding growth factors to the microspheres [165].

Gelatin microspheres are useful for delivery of growth factors due to the availability of gelatin with net positive or net negative charge, with controlled delivery based on electrostatic interactions. A representative gelatin inverse suspension crosslinking protocol is described. An aqueous solution of gelatin at 40°C was added dropwise to stirred olive oil at 40°C. The suspension was then cooled to 15°C to solidify the aqueous gelatin phase. The microspheres were washed with acetone and isopropanol at 4°C to remove the olive oil. The microspheres were then crosslinked in water containing glutaraldehyde at 4°C for 15 hours while stirring. A solution of glycine was used to block unreacted groups [166]. Using similar protocols, gelatin microspheres were made with anionic gelatin (IEP of 5.0), freeze dried and then swollen in a

solution containing the positively charged growth factors TGF-beta [167–169] or bFGF [170]. Electrostatic interactions controlled the release of the proteins, as decreasing the pH resulted in faster release [169]. Growth factor-loaded gelatin microspheres were mixed with chondrocytes or mesenchymal stem cells and polymerized in oligo(poly(ethylene glycol)-fumarate)/PEG-diacrylate hydrogels (Figure 12C) [168,171–173]. Gelatin microspheres produced by suspension polymerization have been used as porogens in non-hydrogel scaffolds [162].

Similar suspension polymerization protocols have been used to produce gelatin microcarriers for cell culture [174]. To make the microcarriers porous, a ‘double emulsion’ strategy was used. A small amount of toluene was suspended in a gelatin solution at 60°C in the presence of surfactants. This solution was added to excess toluene, stirred and cooled. After glutaraldehyde crosslinking, the beads were autoclaved and washed with water and acetone to remove toluene and surfactants, resulting in highly porous microcarriers [175].

Suspension polymerization/crosslinking of aqueous two phase systems/coacervates

Polymers or biomacromolecules may also be crosslinked within aqueous two phase systems to produce microspheres. Generally, the two aqueous phases are allowed to completely phase separate and then are stirred to make droplets during crosslinking. These are simply suspension polymerizations assuming the monomer/macromonomers prefer one of the phases.

Gelatin at elevated temperatures forms simple coacervates in, for example, ethanol/water mixtures, or complex coacervates in the presence of polyanions such as gum arabic. Following coacervation and stirring, the spherical gelatin-rich domains can be solidified by rapid cooling. To prevent re-dissolution of the gelatin upon heating, the solidified gelatin microparticles may be crosslinked with formaldehyde, glutaraldehyde, etc. Crosslinked gelatin microparticles were originally used to encapsulate reactive molecules that form a colored product upon mixing. These were used to produce ‘carbonless’ carbon paper [176,177]. Dye precursors were separately dissolved in 1,2,3-trichloro-4-phenylbenzene that was emulsified in water containing gum arabic and gelatin. At 50°C with stirring, the gum arabic and gelatin formed a complex coacervate that deposited around the dye/solvent droplets. The solution was poured into ice cold water and the gelatin was crosslinked with formalin at 3°C to produce microcapsules several microns in size. Microcapsules containing one of the reactive molecules were mixed with microcapsules containing the other reactive molecule and coated on sheets of paper. Upon applying pressure, the microcapsules burst, producing a dye at that location. A similar technique has been used with a simple coacervate of gelatin in sodium sulfate solutions [178]. Gelatin coacervates generally prefer to surround and emulsify water-insoluble phases. This property has been exploited for the encapsulation of pharmaceuticals [179]. For example, Jizomoto described the encapsulation of liquid paraffin in gelatin/gum arabic microspheres by complex coacervation. Liquid paraffin containing an oil soluble dye was suspended in an aqueous solution of gum arabic at 55–60°C. Gelatin was then dissolved in the aqueous phase. Gelatin and gum arabic formed a complex coacervate below pH 5, but addition of PEG to the aqueous solution promoted phase separation at a higher pH. The complex coacervate surrounded the liquid paraffin droplets. Cooling to 10°C solidified the complex coacervate, which was then hardened with glutaraldehyde (Figure 13A&B). PEG also causes gelatin to form a simple coacervate that can similarly form microspheres and encapsulate water-insoluble compounds [180,181]. The various gelatin microcapsule production techniques are in essence inverse suspension polymerizations, even though solidification and crosslinking are separate processes. Microparticle formation by coacervation has been reviewed by Arshady [68].

Yin & Stover studied the production of microspheres using a number of copolymers that undergo liquid-liquid phase separations. Coacervation of these copolymers upon heating is different from polymers such as pure poly(NIPAAm) that undergo precipitation upon heating.

Epoxide-containing poly(N,N-dimethylacrylamide- co-glycidyl methacrylate) was synthesized. Raising the temperature of the copolymer dissolved in water resulted in the formation of a coacervate that was broken into droplets by rapid stirring. The epoxide groups on the copolymer were reacted with ethylenediamine to produce microspheres [182]. A copolymer of poly(N,N-dimethylacrylamide-co-allyl methacrylate) was also synthesized that exhibited a cloud point that could be varied between 15–50°C. The copolymer was dissolved below the cloud point, the temperature was raised to phase separate the polymer, which was dispersed by stirring prior to the addition of free radical initiators. The pendant allyl groups were used to crosslink the polymers by free radical polymerization. Microparticles were produced with diameters ranging from 14–72 μm [183]. In another study, a comb copolymer of PEG, styrene and maleic anhydride was incubated with poly(diallyldimethylammonium chloride) to form complex coacervates (carboxylic acids were present in the copolymer due to partial hydrolysis of the anhydride groups). Droplets were produced by stirring and were then crosslinked by reacting polyamines with the remaining anhydride groups [184].

Within a study of suspension polymerization of PEG/methacrylic acid previously discussed, Peppas and colleagues also described the use of an aqueous two phase system for microsphere formation. Phase separation of the polymers was effected using saturated sodium chloride (26 wt%) solutions. PEG-monomethacrylate mixed with tetraethyleneglycol-dimethacrylate was able to form microspheres at 60°C by free radical polymerization with stirring for 18 h. Methacrylic acid microparticles did not form at 60°C but could be produced at 70°C and above, while addition of PEG-monomethacrylate led to the formation of a bulk gel [156]. Irvine and colleagues adapted this protocol to produce PEG microspheres for oligonucleotide delivery. Near saturated solutions of sodium chloride were produced with PEG-monomethacrylate, PEG-dimethacrylate, methacrylic acid, Pluronic F-68 and ovalbumin. At 40°C, a phase separation occurred and polymerization was initiated with APS. In this system, the PEG-methacrylates, the Pluronic F-68 and ovalbumin all may phase separate under these conditions. By itself, Pluronic F-68 formed an emulsion with mean diameter of ≈ 400 nm by light scattering, which did not change over 4 h if the solution was stirred. Addition of PEG macromers or protein had little effect on the size of the phase separated domains. Upon polymerization, 75% of the ovalubumin was incorporated into particles, while only 4% of the PEG macromers was found in the particles. Interestingly, few particles were recovered if the ovalbumin was excluded from the reaction. The size of the formed particles was essentially that of the Pluronic-rich domains in the emulsion, but if the Pluronic concentration was reduced from 4% to 2%, flocs of >10 μm particles formed [185].

Phase separation of PEG in saturated sodium sulfate solutions has been used to increase of mass of reactive PEG bound to a surface. Substrates were plasma coated with N-heptylamine and then reacted with PEG activated with an N-hydroxysuccinimide ester. If the reaction was performed in the sodium sulfate solution, the PEG existed in a phase separated state and encountered the surface due to agitation of the container (the PEG-rich phase is less dense than the PEG-poor phase). By quartz crystal microbalance (QCM), it was found that ‘cloud point conditions’ immobilized almost four times as much PEG on the surface compared to a homogenous solution. Protein adsorption on the PEG layer was undetectable if the PEG was reacted under cloud point conditions [186].

In 1998, Frannssen, Hennick and colleagues described the production of dextran, PEG and gelatin microspheres by aqueous two phase suspension polymerization. For example, dextran-methacrylate at 1%(w/w) was phase separated from a 23%(w/w) PEG mol. wt. 10,000 solution. With vigorous mixing, the dextran-methacrylate was free-radical crosslinked using potassium persulfate to produce ≈ 5 μm microspheres (Figure 14A). Other aqueous two phase systems were also explored. Dextran-methacrylate suspended in Pluronic F68, or PEG-dimethacrylate suspended in dextran produced ≈ 5 μm microspheres. However, when PEG-dimethacrylate

was suspended in 38% magnesium sulfate, large aggregates formed, which was ascribed to the low viscosity of the magnesium sulfate solution. Liquid gelatin solutions were suspended in poly(vinyl pyrrolidone) or dextran at 60°C, forming solid microspheres upon cooling. Additionally, hollow microcapsules were produced by suspending PEG mol. wt. 10,000 in dextran-methacrylate solution, then suspending this emulsion in PEG mol. wt. 4000 [187–189]. The sizes of the microspheres were found to increase as the viscosity of the PEG-rich phase decreased, or as the viscosity of the dextran-rich phase increased. However, if the volume of the PEG-rich phase was greater than 40 times the volume of the dextran-methacrylate-rich phase, microsphere size was independent of the solution viscosity [100].

One potential advantage of dextran microspheres versus PEG microspheres is an enhanced ability to deliver proteins. In the PEG-dextran two phase system, many proteins partition preferentially into the dextran phase [53]. Greater than 80% of IgG added to the PEG/dextran-methacrylate solution became trapped within dextran microspheres. The microspheres were degraded by dextranase to release the protein. Alternatively, microspheres were formed from dextran-hydroxyethylmethacrylate (dextran-HEMA), which has an ester bond that is readily hydrolyzed. Degradation of the microspheres by hydrolysis permitted release of IgG [190] or IL-2 [191]. Liposomes were also found to be efficiently encapsulated in dextran microspheres [192].

Scaffolds have been produced by assembling the dextran-based microspheres. Charge was added to the dextran-HEMA microspheres by copolymerization with methacrylic acid (negative) or dimethylaminoethyl methacrylate (positive). Microspheres of opposite charges were dried, mixed and reswelled in protein-containing solutions. A microsphere-based scaffold formed due to electrostatic interactions between the oppositely charged microspheres (Figure 14B). Smaller proteins entered the microspheres, while larger proteins remained trapped between the microspheres [193, 194]. By increasing the volume fraction of microspheres in the solution during assembly, the storage modulus of the scaffolds could be greatly increased [195]. Smaller microspheres of opposite charge (7 μm average diameter) assembled into stronger scaffolds than those assembled from larger microspheres (20 μm average diameter). As the solids content increased from 15% to 25%, the storage modulus of the small microsphere scaffolds increased from about 4000 to about 30,000 Pa. At 15% solids, the highest strength scaffolds were produced when small negatively charged microspheres were mixed with large positively charged microspheres at a weight ratio of 3:1 of small:large microspheres. If the weight ratio of small to large microspheres was reversed, no scaffold formed. This was consistent with intuition that one large microsphere may interact with many small microspheres. Scaffolds with storage moduli $<\approx$ 4000 Pa could be flowed through a 25 gauge syringe needle to form a continuous fiber. This suggested the possibility of delivering a microsphere-based scaffold by injection [196]. The dextran microspheres were also modified with L-oligolactate chains or D-oligolactate chains. Upon mixing, stereocomplexation of the oligolactides with opposite chirality produced scaffolds with storage moduli up to 12.5 kPa. Entrapment of lysozyme within or between the microspheres during scaffold formation resulted in controlled release over a period of days/weeks [197].

Inspired by the lipid-encapsulated microspheres of Kiser et al., degradable dextran microspheres produced by suspension in PEG solutions were encapsulated with lipids and/or polyelectrolyte multilayers and exploded during the degradation of the crosslinked dextran (Figure 14D). The charge on the surface of the microspheres was chosen to be opposite the charge on the lipid headgroup, either by copolymerization with charged monomers or by first coating the microspheres with polyelectrolyte mulitlayers. Degradation of the ester bonds in the dextran microgels in basic solutions caused an increase in osmotic pressure that burst the lipid coating [198]. The lipid coating was not needed if the polyelectrolyte coating was covalently crosslinked. However, it was found that 15 μm microspheres were not able to

generate high enough osmotic pressures to rupture the crosslinked capsule. Large dextran-HEMA microspheres (150 μm in diameter) were thus produced by slowly dropping a dextran-HEMA solution into a stirred vessel containing a PEG solution. The larger microspheres were able to burst the crosslinked electrolyte multilayer, allowing rapid release of smaller microcarriers or nanoparticles [199, 200]. The nanoparticles were ejected forcefully enough to travel 400 μm in 40 seconds [200].

Aqueous two phase systems have been further explored for the production of PEG microspheres. Degradable, methacrylated PEG derivates were suspended in dextran solutions and free radical crosslinked. Copolymerization with charged monomers allowed the formation of lipid bilayers or multilayers around the formed microspheres, via interaction of the charged headgroup on the lipid with the oppositely charged microsphere [201]. Chu and colleagues produced PEG-diacrylate/NIPAAm microspheres by suspension polymerization in magnesium sulfate solutions. The gel precursors were phase separated from water using 30% (w/w) magnesium sulfate. A bimodal distribution of particle sizes was observed, with 60% of the microspheres around 50 μm and rest in the range of 3–10 μm [202]. The bimodal distribution suggests two simultaneous polymerization mechanisms, perhaps a suspension polymerization and a precipitation polymerization. The microgels were then incorporated as part of the structure of bulk NIPAAm hydrogels, with the microgels increasing the swelling/deswelling rates of the hydrogels [203].

Phase inversion - ‘Pinning’ of phase separations in unstirred systems

Phase inversion may be used to directly form porous materials, particularly asymmetric membranes for separation processes [204–206], or non-hydrogel scaffolds for tissue engineering [207]. Asymmetric porous membranes are typically formed by adding a liquid polymer solution coated on a substrate to a bath of non-solvent (immersion precipitation). Typically, evaporation before immersion results in the formation of a non-porous skin that controls the separation process. After immersion, the non-solvent diffuses into the polymer solution and a χ-induced phase separation takes place, followed by solidification before complete phase separation occurs. The polymer may solidify due to crystallization, vitrification (formation of an amorphous solid below the glass transition temperature), or gelation (the formation of chemical or physical crosslinks) [204,205]. Alternatively, a thermally induced phase separation with a deep quench to a low temperature may also result in solidification shortly after phase separation [204,205]. Hashimoto pointed out the similarities between spontaneous pinning at the percolation-to-cluster transition and pinning by crystallization, vitrification or gelation. In all cases, coarsening, as measured by light scattering or other means, slows dramatically or even halts [57].

Phase inversion by immersion precipitation—Phase inversion techniques have also been used to produce membranes for biomedical applications, typically by immersion precipitation. Originally, poly(vinyl alcohol) hydrogel membranes were produced for a variety of separation processes, e.g desalination or waste water remediation [208,209]. Asymmetric PVA membranes were produced by casting an aqueous poly(vinyl alcohol) solution on a plate, which was immersed into a precipitating bath containing acetone [209], or aqueous solutions with high concentrations of sulfate ions [208,210,211]. The membranes were stabilized by drying [208], crosslinking with formaldehyde [210] or glutaraldehyde [211], or complexation with boronate ions [209]. Brannon & Peppas used a drying step prior to precipitation to increase the thickness of the skin layer and the membranes showed some selectivity between theophylline and vitamin B_{12} [211].

Sefton and colleagues explored phase inversion to form porous microcapsules around living cells, using a copolymer of HEMA and methyl methacrylate that precipitated in water. The

copolymer was dissolved in PEG mol. wt. 200 and extruded into an aqueous solution to cause precipitation of the copolymer. Red blood cells were encapsulated in the large microcapsules by co-extrusion in a coaxial geometry. The walls of the microcapsules generally had smooth-surfaced skins with finger-like macrovoids within the walls (Figure 15) [212, 213]. Such structures are typical in membranes formed by immersion precipitation.

Phase inversion of AN-69, a copolymer of acrylonitrile and sodium methallyl sulphonate, also produces porous membranes and hydrogels. AN-69 was dissolved in DMSO and flowed coaxially with saline. The solution was dropped into a saline bath, causing the copolymer to precipitate as the DMSO became diluted with water. The hydrophilic hollow fibers that formed were porous and permeable to albumin but not IgG. Hepatocytes cultured in the hollow fibers secreted albumin for longer periods compared to those cultured in a Petri dish [214]. The same copolymer dip-coated on a glass slide produced a hydrogel upon immersion in saline. The hydrogel was used for the culture of corneal epithelial cells [215].

Pinning following thermally induced phase separations—Solid gelatin hydrogels may be produced by thermally inducing phase separation and then pinning the coarsening process by cooling below the solidification temperature. Gelatin and dextran (both at 4.2% (w/w)) were dissolved in 0.5 M sodium chloride. Under these conditions, the two phase system has a UCST at about 38°C, while the gelatin solidifies at about 25°. Solutions that were heated to 45°C were homogenous. When cooled to 30°C, an aqueous two phase system formed and thee phase-separated domains rapidly evolved to form gelatin-rich droplets (Figure 16A&B). However, if the solution at 45°C was cooled to 21°C, coarsening was halted at an early stage by solidification of the gelatin (Figure 16C). The hydrogel that formed had a reticulated (net-like) structure of bicontinuous phases, which are expected to be present during the early stages of spinodal decomposition. Light scattering of the solution cooled to 30°C showed the typical pattern for spinodal decomposition. A broad peak at a high scattering wave vector (q) sharpened and moved to smaller values of q over time. The shift of the peak to lower q was consistent with coarsening, with the size of the scattering domains increasing over time (Figure 16D). The solution that was cooled to 21°C showed a similar pattern until about 10 min after the temperature change, after which time the peak value for q remained essentially constant (Figure 16E). Thus, the system was pinned at an early stage of phase separation, prior to the percolation-to-cluster transition (Figure 16F) [216].

Moeller and colleagues rapidly froze solutions of PEG and HEMA/ethylene glycol dimethacrylate to pin the bicontinuous structure present at the early stages of spinodal decomposition. The solutions were cooled to −180°C at a rate of 1200 K/min. The PEG began to phase separate and then crystallized. The phase-separated structures were further stabilized by polymerizing the HEMA/ethylene glycol dimethacrylate. The PEG was found to exist as strands about 10 nm in diameter. If the solutions were cooled more slowly, larger, spherical PEG domains were observed. Thus, by rapid cooling, the polymerization pinned the phase separation prior to the percolation-to-cluster transition [217,218].

Anseth and colleagues dissolved methacrylated gelatin at 60°C and then rapidly photopolymerized the solution between glass plates. A porous hydrogel was formed, which was suggested to result from phase separation during crosslinking. Although only analyzed by SEM, lower concentrations of initiator led to larger pores, consistent with increased coarsening for longer times to reach the gel point [219]. The mechanism of pore formation was not studied, but the authors suggested that ν-induced microsyneresis caused the phase separation. As in all microsyneresis phenomena, the solvent-rich pores coarsen over time but become trapped due to gelation, and thus microsyneresis represents a pinning process if the solution is unmixed. More detailed study of this and other hydrogel systems will be required to understand the thermodynamics and kinetics of phase separation and the role of drying artifacts in producing

the pore structures observed by SEM [220–222]. Scanning confocal fluorescence microscopy may be of utility.

Formation of microspheres by the pinning of unstirred phase separating solutions is also possible. To do so requires rapid gelation of polymer-rich droplets soon after the percolation-to-cluster transition. The author's group recently described a method to produce PEG microspheres in the micron range by precisely timing gelation to occur soon after a thermally induced phase separation. Eight arm PEG-vinylsulfone was first reacted with eight arm PEG-amine in aqueous solution. Progress towards gelation was monitored by dynamic light scattering. Before the gel point was reached, the reacting PEG solution was diluted and cooled to room temperature. Sodium sulfate was added at a concentration that did not cause phase separation of the PEG at room temperature. After mixing, the homogenous solutions were heated to 37°C or higher to effect a thermally induced phase separation. The solutions were not mixed during heating, such that growth of the phase separated domains was as slow as possible. If the solutions reached the gel point soon after phase separation, spherical hydrogel microspheres were produced (Figure 17A). The polydispersity in size was about 3.0, which was consistent with the predicted polydispersity of unmixed phase separated systems coarsening by coalescence or Ostwald ripening.

The buoyancy and sizes of the microspheres could be controlled independently. The size of the microspheres could be controlled by changing the time to reach the gel point following phase separation. This was varied by pre-reacting the samples prior to phase separation or by changing the pH or temperature. Buoyancy was determined by the degree of swelling of the microspheres after buffer exchange into PBS, which was a function of crosslink density. The crosslink density was controlled by the length of time that the microspheres were incubated beyond the gel point in the phase separated state. Increased crosslinking beyond the gel point decreased swelling and buoyancy [223]. Scanning confocal microscopy revealed solvent-rich pores within the microspheres, most likely a result of ν-induced microsyneresis (Figure 17B).

The microspheres were washed with buffer to remove sodium sulfate and crosslinked to form scaffolds in the presence of cells. Microspheres came together to form scaffolds by reacting with proteins in serum-containing medium (Figure 17C). Microspheres made by crosslinking eight arm PEG-acrylate with eight arm PEG-amine were used as porogens, which dissolved within two days by hydrolysis of ester bonds. Dissolution of the porogenic microspheres within the scaffold had little effect on the viability of cells in the scaffold (Figure 17D). Microspheres made by reacting eight arm PEG-vinylsulfone with albumin were used to deliver the bioactive lipid sphingosine 1-phosphate to promote endothelial cell migration into the macropores formed by the porogenic microspheres [224].

Emulsion/interfacial polymerization of hydrophilic polymers

Inverse emulsion polymerization of hydrophilic macromonomers, in which the initiator is in the organic phase, is less straightforward than inverse suspension polymerization. Inverse emulsion polymerizations with low molecular weight monomers such as acrylamide or acrylic acid have been extensively studied. Kissel and colleagues compared the effects of water-soluble and water-insoluble initiators on the polymerization of acrylic acid. With ammonium persulfate, micron-sized particles were obtained, consistent with inverse suspension polymerization. With AIBN, nano-scale particles were obtained, consistent with inverse emulsion polymerization [225]. Although this is the expected behavior, this has proven to be exceptional with inverse systems, largely because the commonly used surfactants produce microemulsions (discussed below) [20,226].

The difficulties of water-in-oil polymerizations may be overcome by performing a standard oil-in-water emulsion polymerization with some small amount of a hydrophilic co-monomer.

Hydrophilic monodisperse poly(styrene-*co*-methacrylic acid) microspheres were produced by emulsion polymerization, with a mean diameter about 200 nm. These particles were added to water, which was then suspended in toluene. Upon heating to 105°C, the monodisperse particles fused to form about 30 μm particles with a polydispersity in size typical of suspension polymerization. The secondary particles were porous due to spaces between the primary particles [227]. Saunders and colleagues used oil-in-water emulsion polymerization to produce microspheres containing methyl methacrylate, methacrylic acid and ethylene glycol dimethacrylate. The liquid monomers were mixed and added to an aqueous solution containing SDS. Direct emulsion polymerization of the mixture was performed using APS as the water-soluble initiator. After formation of the initial particles ('seed' stage), a second batch of initiator was added to produce larger particles ('feed' stage). The microspheres were in a deswollen state due to protonated acid groups. Degenerated intervertebral discs were replaced by injecting a dispersion of microspheres into the tissue. The microspheres swelled at physiological pH by deprotonation of the acid groups [228–230].

The analog of emulsion polymerization for polycondensation/polyaddition polymerizations is interfacial polymerization. Kabanov and colleagues produced nanogels by reacting poly (ethylenimine) dissolved in water with activated PEG dissolved in dichloromethane. The solution was mixed, but the polymers remained predominantly in separate phases because of the charge on the poly(ethylenimine) and the high degree to which PEG partitions to DCM from water. Presumably, the PEG and PEI reacted at the interface between the water and dichloromethane phases. The produced 'nanogels' were present in three size ranges, with the majority in the range of 150–240 nm [231,232]. Gelatin microcapsules have also been crosslinked in the presence of living cells via an interfacial polymerization by Mikos and colleagues. Gelatin and rat marrow stromal cells were mixed at 37°C and dropped into chilled mineral oil with stirring. The amine-crosslinking reagent dithiobis(succinimidylpropionate) was present in the oil phase, resulting in an interfacial polymerization (Figure 18). The crosslinking at the interface produced hollow capsules containing cells, which protected the cells during polymerization of poly(propylene fumarate) and simultaneously served as porogens [233–235].

Inverse micro/miniemulsion polymerization

Microemulsion polymerizations occur in thermodynamically stable emulsions. The initiator may be present in the same phase as the monomer as in a suspension polymerization, but the kinetics are typically similar to emulsion polymerization due to the low mean number of radicals per micelle. The term 'microsuspension polymerization' is only used if initiation is in the monomer-rich droplets and the kinetics are known to be consistent with greater than one radical per micelle [20]. Polymerization within inverse micro/miniemulsions to produce nanogels and microgels has been reviewed [236], and only a few examples will be described to illustrate the principle.

To produce small hydrogel particles, van Thienen et al. encapsulated methacrylated PEG or dextran in liposomes and performed an inverse microemulsion polymerization. Not all of the macromer was encapsulated, but upon dilution, only the solution inside the liposomes gelled during photopolymerization. The 'nanogels' produced were about 400–600 nm in diameter. The 'nanogels' showed controlled release of bovine serum albumin over a period of about 7 days [201,237,238].

The free radical polymerization of Pluronics in micelles yields nanogels or microgels. For example, Tirrelli and colleagues conducted a water-in-oil photopolymerization of the PEG-containing surfactant Pluronic F127. Aqueous solutions of Pluronic F127-diacrylate, PEG-diacrylate, triethanolamine and eosin Y were dispersed by sonication in hexane using the surfactant Span 65. Microgels with average diameters by light scattering of a few hundred

nanometers were produced, which gelled upon raising the temperature above the LCST of Pluronic F127. While solutions of Pluronic F127 also gel above the LCST, microgel-containing solutions dissolved much more slowly upon temperature decrease. Such materials may be useful in developing injectable hydrogels [239]. The anti-cancer agent doxorubicin was incorporated in the microgels, exhibiting controlled release of the drug [240,241]. Similarly, Yang and Ding acrylated Pluronic F127 that had been chain extended with lactide groups. The macromonomer was dissolved above the CMC as assessed by pyrene fluorescence. APS was used to crosslink polymer in the micelles at 40°C. The final product had an average hydrodynamic radius of about 32 nm below the LCST of Pluronic F127. Above the LCST (at 37°C), the mean nanogel size decreased to about 15 nm. Unpolymerized Pluronic macromer was about 12 nm in size at all temperatures. The nanogel solutions gelled above the LCST of Pluronic F127 at concentrations of about 16 wt% and greater, while the unpolymerized macromonomer only gelled above about 25 wt% [242]. The difference in size between these two types of Pluronic-based nanogels and microgels may be because the former may actually be a miniemulsion polymerization. This illustrates the difficulty encountered in classifying such reactions.

In miniemulsion polymerizations, the initiator may be in either phase, with kinetics showing mixed emulsion/suspension character. Due to the small size and large surface area of the monomer droplets, initiation occurs within the monomer droplets even if the initiator is in the continuous phase [25]. As an example, atom transfer radical polymerization of oligoethyleneglycol-dimethacrylate was conducted in a kinetically stable inverse miniemulsion. The macromonomer and the other reagents were dissolved in water and added to cyclohexane with Span 80 as the surfactant. The solution was sonicated to produce the inverse miniemulsion. Polymerization commenced with addition of ascorbic acid [243].

Another related class of heterogeneous polymerization relies on spontaneously formed emulsions, which do not require input of mechanical energy [244]. Pluronic solutions may spontaneously form kinetically stable ‘nanoemulsions’ by taking advantage of the LCST properties of these surfactants. At elevated temperatures, the hydrophilic and lipophilic natures of the surfactant are balanced and bicontinuous oil/water phases may spontaneously form. With rapid cooling, the hydrophilic portion of the surfactant becomes more hydrated and the bicontinuous phase breaks up into kinetically stable droplets with diameters between 50–500 nm [245]. This is akin to a percolation-to-cluster transition, with the formed clusters stabilized by steric stabilization due to the surfactant. Another method to produce kinetically stable emulsions without mixing is the solvent displacement method or ‘ouzo effect’. A binary system (e.g. the water-insoluble molecule anethol in ethanol in the case of ouzo) is diluted with a third component (e.g. water in the case of ouzo) until a phase separation occurs. If the solutions are stabilized against coalescence by electrostatic or steric stabilization, slow rates of coarsening are observed. Such ‘phase inversion temperature’ methods and ‘solvent displacement’ methods have been widely used in the pharmaceutical industry to produce optically clear, kinetically stable dispersions, and polymerization within the stable phase is possible [244].

Ionotropic gelation

A remarkable type of phase separation occurs within alginate scaffolds. ‘Ionotropic gelation’ produces honeycomb-shaped parallel channels that extend the entire length of the scaffold (Figure 19). The channels form when an alginate-coated vessel is filled with a liquid alginate solution and calcium chloride is sprayed on top to produce a thin gel layer, which is then overlayed with calcium chloride solution. Overnight, the honeycomb pattern emerges. The structure develops due to syneresis of the forming gel, which places stress in a single plane (the diffusion front of the calcium ions) as the hydrogel contracts. The emergence of the

honeycomb structure presumably minimizes these stresses, although rigorous theoretical analysis has not been performed [246–248].

Cryogelation

Liquid-liquid phase separation might occur during cryogel formation protocols. Cryogels rely on the formation of solvent crystals to serve as porogens and to concentrate monomers/polymers/macromonomers. For example, if aqueous solutions of poly(vinyl alcohol) are frozen, the ice crystals that form exclude and thus concentrate the polymer. Extensive hydrogen bonds form between the poly(vinyl alcohol) chains and serve as physical crosslinks that persist upon thawing the solution [249]. The ice crystals might solely serve as solid porogens, although phase separation may occur in the concentrated and cooled polymer-rich solution. Water-soluble polymers are known to undergo phase separations upon cooling [54]. However, this temperature is often less than the freezing point of water, and elevated pressures are needed to form liquid-liquid two phase systems [52].

Concluding remarks

A wide variety of polymerization techniques exist to produce hydrogel microspheres and macroporous scaffolds using liquid-liquid phase separated systems. The broad literature across multiple disciplines creates real peril of ‘reinventing the wheel’. Yet, armed with knowledge of the early history and terminology, rapid progress in the application of such techniques in regenerative medicine seems likely.

Acknowledgments

This work was supported by NIH R01HL085364.

References

1. Chung HJ, Park TG. Surface engineered and drug releasing pre-fabricated scaffolds for tissue engineering. Advanced Drug Delivery Reviews 2007;59:249–262. [PubMed: 17482310]
2. Karageorgiou V, Kaplan D. Porosity of 3D biomaterial scaffolds and osteogenesis. Biomaterials 2005;26:5474–5491. [PubMed: 15860204]
3. Mikos AG, Temenoff JS. Formation of highly porous biodegradable scaffolds for tissue engineering. EJB Electronic Journal of Biotechnology 2000;3:114–119.
4. Rivest C, Morrison DWG, Ni B, Rubin J, Yadav V, Mahdavi A, et al. Microscale hydrogels for medicine and biology: Synthesis, characteristics and applications. Journal of Mechanics of Materials and Structures 2007;2:1103–1119.
5. Khademhosseini A, Langer R. Microengineered hydrogels for tissue engineering. Biomaterials 2007;28:5087–5092. [PubMed: 17707502]
6. Jagur-Grodzinski J. Polymers for targeted and/or sustained drug delivery. Polym Adv Technol 2009;20:595–606.
7. Oh JK. Engineering of nanometer-sized cross-linked hydrogels for biomedical applications. Can J Chem-Rev Can Chim 2010;88:173–184.
8. Zhang S. Fabrication of novel biomaterials through molecular self-assembly. Nat Biotechnol 2003;21:1171–1178. [PubMed: 14520402]
9. Graham NB, Cameron A. Nanogels and microgels: The new polymeric materials playground. Pure and Applied Chemistry 1998;70:1271–1275.
10. Funke W, Okay O, Joos-Muller B. Microgels - Intramolecularly crosslinked macromolecules with a globular structure. Advances in Polymer Science 1998;136:139–234.
11. Saunders BR, Laajam N, Daly E, Teow S, Hu XH, Stepto R. Microgels: From responsive polymer colloids to biomaterials. Adv Colloid Interface Sci 2009;147–148:251–262.

12. Saunders BR, Vincent B. Microgel particles as model colloids: theory, properties and applications. Adv Colloid Interface Sci 1999;80:1–25.
13. Arshady R. Suspension, Emulsion, and Dispersion Polymerization - a Methodological Survey. Colloid and Polymer Science 1992;270:717–732.
14. Arshady R, George MH. Suspension, Dispersion, and Interfacial Polycondensation - a Methodological Survey. Polymer Engineering and Science 1993;33:865–876.
15. Schildknecht, CE. Polymer Processes. New York: Interscience Publishers; 1956.
16. Sawhney AS, Pathak CP, Hubbell JA. Bioerodible Hydrogels Based on Photopolymerized Poly (Ethylene Glycol)-Co-Poly(Alpha-Hydroxy Acid) Diacrylate Macromers. Macromolecules 1993;26:581–587.
17. Lutolf MP, Hubbell JA. Synthesis and Physicochemical Characterization of End-Linked Poly (ethylene glycol)-co-peptide Hydrogels Formed by Michael-Type Addition. Biomacromolecules 2003;4:713–722. [PubMed: 12741789]
18. DeForest CA, Polizzotti BD, Anseth KS. Sequential click reactions for synthesizing and patterning three-dimensional cell microenvironments. Nature materials 2009;8:659–664.
19. Smith WV, Ewart RH. Kinetics of emulsion polymerization. Journal of Chemical Physics 1948;16:592–599.
20. Hunkeler D, Candau F, Pichot C, Hemielec AE, Xie TY, Barton J, et al. Heterophase Polymerizations - a Physical and Kinetic Comparison and Categorization. ADVANCES IN POLYMER SCIENCE 1994;112:115–133.
21. Ugelstad J, Kaggerud KH, Hansen FK, Berge A. Absorption of low molecular weight compounds in aqueous dispersions of polymer-oligomer particles, 2. A two step swelling process of polymer particles giving an enormous increase in absorption capacity. Die Makromolekulare Chemie 1979;180:737–744.
22. Vanderhoff JW, Elaasser MS, Micale FJ, Sudol ED, Tseng CM, Silwanowicz A, et al. Preparation of Large-Particle-Size Monodisperse Latexes in Space - Polymerization Kinetics and Process-Development. Journal of Dispersion Science and Technology 1984;5:231–246.
23. Saliakas V, Kotoulas C, Meimaroglou D, Kiparissides C. Dynamic evolution of the particle size distribution in suspension polymerization reactors: A comparative study on Monte Carlo and sectional grid methods. Can J Chem Eng 2008;86:924–936.
24. Smith WV, Ewart RH. Kinetics of emulsion polymerization. J Chem Phys 1948;16:592–599.
25. Lovell, PA.; El-Aasser, MS., editors. Emulsion Polymerization and Emulsion Polymers. West Sussex: John Wiley & Sons, Ltd.; 1997.
26. Pross A, Platkowski K, Reichert KH. The inverse emulsion polymerization of acrylamide with pentaerythritolmyristate as emulsifier - .1. Experimental studies. Polymer International 1998;45:22–26.
27. Vanderhoff JW, Distefano FV, Elaasser MS, Oleary R, Shaffer OM, Visioli DL. Inverse Emulsion Polymerization of Acrylamide - Polymerization Kinetics and Process-Development. Journal of Dispersion Science and Technology 1984;5:323–363.
28. Flory PJ. Thermodynamics of high polymer solutons. J Chem Phys 1942;10:51–61.
29. LaMer VK, Dinegar RH. Theory, Production and Mechanism of Formation of Monodispersed Hydrosols. Journal of the American Chemical Society 1950;72:4847–4854.
30. Barrett, KEJ., editor. Dispersion Polymerization in Organic Media. London: John Wiley & Sons; 1975.
31. Metanomski, WV. Compendium of Macromolecular Nomenclature: The Purple Book. Oxford: Blackwell Science; 1991.
32. Aleman J, Chadwick AV, He J, Hess M, Horie K, Jones RG, et al. Definitions of terms relating to the structure and processing of sols, gels, networks, and inorganic-organic hybrid materials (IUPAC Recommendations 2007). Pure and Applied Chemistry 2007;79:1801–1827.
33. Baker WO. Microgel, A New Macromolecule - Relation to sol and gel as structural elements of synthetic rubber. Industrial and Engineering Chemistry 1949;41:511–520.
34. Flory PJ. Molecular Size Distribution in Three Dimensional Polymers. I. Gelation. J Am Chem Soc 1941;63:3083–3090.

35. Stockmayer WH. Theory of molecular size distribution and gel formation in branched-chain polymers. J Chem Phys 1943;11:45–55.
36. Horie K, Baron M, Fox RB, He J, Hess M, Kahovec J, et al. Definitions of terms relating to reactions of polymers and to functional polymeric materials - (IUPAC Recommendations 2003). Pure Appl Chem 2004;76:889–906.
37. Langer R, Peppas N. Chemical and Physical Structure of Polymers as Carriers for Controlled Release of Bioactive Agents - a Review. Journal of Macromolecular Science-Reviews in Macromolecular Chemistry and Physics 1983;C23:61–126.
38. Chen J, Park H, Park K. Synthesis of superporous hydrogels: hydrogels with fast swelling and superabsorbent properties. J Biomed Mater Res 1999;44:53–62. [PubMed: 10397904]
39. Stockmayer WH, Schmidt M. Effects of Polydispersity, Branching and Chain Stiffness on Quasi-Elastic Light-Scattering. Pure and Applied Chemistry 1982;54:407–414.
40. Berne, BJ.; Pecora, R. Dynamic light scattering: with applications to chemistry, biology, and physics. Mineola, NY: Dover Publications; 2000.
41. Dill, KA.; Bromberg, S. Molecular Driving Forces: Statistical Thermodynamics in Chemistry & Biology. New York: Garland Science; 2003.
42. Rubinstein, M.; Colby, RH. Polymer Physics. New York: Oxford University Press; 2003.
43. Inoue T. Reaction-Induced Phase-Decomposition in Polymer Blends. Prog Polym Sci 1995;20:119–153.
44. Heskins M, Guillet JE. Solution properties of Poly(N-isopropylacrylamide). J Macromolec Sci, Part A 1968;2:1441–1455.
45. Bailey FE, Callard RW. Some properties of poly(ethylene oxide) in aqueous solution. J Appl Polym Sci 1959;1:56–62.
46. Kjellander R, Florin E. Water-structure and changes in thermal-stability of the system poly(ethylene oxide)-water. Journal of the Chemical Society-Faraday Transactions I 1981;77:2053.
47. Matsuyama A, Tanaka F. Theory of solvation-induced reentrant phase separation in polymer solutions. Physical Review Letters 1990;65:341. [PubMed: 10042894]
48. Saeki S, Kuwahara N, Nakata M, Kaneko M. Upper and lower critical solution temperatures in poly (ethylene glycol) solutions. Polymer 1976;17:685688.
49. Zhang YJ, Cremer PS. Interactions between macromolecules and ions: the Hofmeister series. Current Opinion in Chemical Biology 2006;10:658–663. [PubMed: 17035073]
50. Hey MJ, Jackson DP, Yan H. The salting-out effect and phase separation in aqueous solutions of electrolytes and poly(ethylene glycol). Polymer 2005;46:2567–2572.
51. Cook RL, King HE, Peiffer DG. Pressure-Induced Crossover from Good to Poor Solvent Behavior for Polyethylene Oxide in Water. Physical Review Letters 1992;69:3072–3075. [PubMed: 10046718]
52. Sun T, King HE. Discovery and modeling of upper critical solution behavior in the poly(ethylene oxide) water system at elevated pressure. Macromolecules 1998;31:6383–6386.
53. Albertsson, PA. Partition of cell particles and macromolecules. New York: Wiley; 1986.
54. Molyneux, P. Water-soluble synthetic polymers: Properties and behavior. Vol. Vol. I. Boca Raton: CRC Press; 1983.
55. Siggia ED. Late stages of spinodal decomposition in binary mixtures. Physical Review A 1979;20:595.
56. Crist B. On "pinning" domain growth in two-phase polymer liquids. Macromolecules 1996;29:7276–7279.
57. Hashimoto, T. Structure of Polymer Blends. In: Cahn, RW.; Haasen, P.; Kramer, EJ., editors. Materials Science and Technology: A Comprehensive Treatment, Vol 12. Weinheim: VCH; 1993.
58. Takeno H, Iwata M, Takenaka M, Hashimoto T. Combined light scattering and laser scanning confocal microscopy studies of a polymer mixture involving a percolation-to-cluster transition. Macromolecules 2000;33:9657–9665.
59. Utracki, LA. Polymer Blends Handbook. Dordrecht: Kluwer; 2002.
60. Cahn JW, Hilliard JE. Free energy of a nonuniform system. I. Interfacial free energy. J Chem Phys 1958;28:258–267.

61. Chen LQ, Shen J. Applications of semi-implicit Fourier-spectral method to phase field equations. Comput Phys Commun 1998;108:147–158.
62. Flory PJ, Rehner J. Statistical Mechanics of Cross-Linked Polymer Networks II. Swelling. J Chem Phys 1943;11:521–526.
63. Dusek, K. Inhomogeneities induced by crosslinking in the course of crosslinking copolymerization. In: Chompff, AJ.; Newman, S., editors. Polymer networks: Structure and mechanical properties. New York: Plenum Press; 1971.
64. Okay O. Macroporous copolymer networks. Prog Polym Sci 2000;25:711–779.
65. Kruyt, HR. Colloid Science, II Reversible systems. New York: Elsevier; 1949.
66. Everett DH. Manual of Symbols and Terminology for Physicochemical Quantities and Units, Appendix II: Definitions, Terminology and Symbols in Colloid and Surface Chemistry. Pure Appl Chem 1972;31:577–638.
67. Russel, WB.; Saville, DA.; Schowalter, WR. Colloidal Dispersions. Cambridge: Cambridge University Press; 1989.
68. Arshady R. Microspheres and microcapsules, a survey of manufacturing techniques .2. coacervation. Polym Eng Sci 1990;30:905–914.
69. Wichterle O, Lim D. Hydrophilic gels for biological use. Nature 1960;185:117–118.
70. Wichterle, O.; Lim, D., inventors. Process for producing shaped articles from three-dimensional hydrophilic high polymers patent US. 2,976,576. 1961.
71. Wichterle, O.; Lim, D., inventors. Cross-linked hydrophilic polymer and articles made therefrom patent US. 3,220,960. 1965.
72. Dusek K, Sedlacek B. Structure and properties of hydrophilic polymers and their gels XI. Microsyneresis in swollen poly(ethylene glycol methacrylate) gels induced by changes in temperature. Collection Czechoslov Chem Commun 1968;34:136–157.
73. Weaver JVM, Bannister I, Robinson KL, Bories-Azeau X, Armes SP, Smallridge M, et al. Stimulus-responsive water-soluble polymers based on 2-hydroxyethyl methacrylate. Macromolecules 2004;37:2395–2403.
74. Barvic M, Kliment K, Zavadil M. Biologic properties and possible uses of polymer-like sponges. Journal of biomedical materials research 1967;1:313–323. [PubMed: 5605620]
75. Sprincl L, Kopecek J, Lim D. Effect of porosity of heterogeneous poly(glycol monomethacrylate) gels on the healing-in of test implants. Journal of biomedical materials research 1971;5:447–458. [PubMed: 5120385]
76. Brauker JH, Carr-Brendel VE, Martinson LA, Crudele J, Johnston WD, Johnson RC. Neovascularization of synthetic membranes directed by membrane microarchitecture. Journal of biomedical materials research 1995;29:1517–1524. [PubMed: 8600142]
77. Sieminski AL, Gooch KJ. Biomaterial-microvasculature interactions. Biomaterials 2000;21:2232–2241. [PubMed: 11026629]
78. Ronel SH, D'Andrea MJ, Hashiguchi H, Klomp GF, Dobelle WH. Macroporous hydrogel membranes for a hybrid artificial pancreas. I. Synthesis and chamber fabrication. J Biomed Mater Res 1983;17:855–864. [PubMed: 6619181]
79. Klomp GF, Hashiguchi H, Ursell PC, Takeda Y, Taguchi T, Dobelle WH. Macroporous hydrogel membranes for a hybrid artificial pancreas. II. Biocompatibility. J Biomed Mater Res 1983;17:865–871. [PubMed: 6413510]
80. Obaidat AA, Park K. Characterization of protein release through glucose-sensitive hydrogel membranes. Biomaterials 1997;18:801–806. [PubMed: 9177859]
81. Kliment K, Stol M, Fahoun K, Stockar B. Use of spongy hydron in plastic surgery. J Biomed Mater Res 1968;2:237–243. [PubMed: 5707847]
82. Kon M, de Visser AC. A poly(HEMA) sponge for restoration of articular cartilage defects. Plastic and reconstructive surgery 1981;67:288–294. [PubMed: 7232561]
83. Cifkova I, Sprincl L. The use of 99Tc-pyrophosphate for imaging and measuring of calcification caused by implanted polymers. J Biomed Mater Res 1980;14:723–730. [PubMed: 6300131]
84. Imai Y, Masuhara E. Long-term in vivo studies of poly(2-hydroxyethyl methacrylate). J Biomed Mater Res 1982;16:609–617. [PubMed: 7130216]

85. Sprincl L, Vacik J, Kopecek J. Biological tolerance of ionogenic hydrophilic gels. J Biomed Mater Res 1973;7:123–136. [PubMed: 4691155]

86. Hicks CR, Crawford GJ, Lou X, Tan DT, Snibson GR, Sutton G, et al. Corneal replacement using a synthetic hydrogel cornea, AlphaCor: device, preliminary outcomes and complications. Eye (London, England) 2003;17:385–392.

87. Dziubla TD, Torjman MC, Joseph JI, Murphy-Tatum M, Lowman AM. Evaluation of porous networks of poly(2-hydroxyethyl methacrylate) as interfacial drug delivery devices. Biomaterials 2001;22:2893–2899. [PubMed: 11561895]

88. Dziubla TD, Lowman AM. Vascularization of PEG-grafted macroporous hydrogel sponges: a three-dimensional in vitro angiogenesis model using human microvascular endothelial cells. Journal of biomedical materials research 2004;68:603–614. [PubMed: 14986316]

89. Chen X, Aledia AS, Ghajar CM, Griffith CK, Putnam AJ, Hughes CC, et al. Prevascularization of a fibrin-based tissue construct accelerates the formation of functional anastomosis with host vasculature. Tissue engineering 2009;15:1363–1371. [PubMed: 18976155]

90. Luo Y, Dalton PD, Shoichet MS. Investigating the Properties of Novel Poly(2-hydroxyethyl methacrylate-co-methyl methacrylate) Hydrogel Hollow Fiber Membranes. Chemistry of Materials 2001;13:4087–4093.

91. Dalton PD, Flynn L, Shoichet MS. Manufacture of poly(2-hydroxyethyl methacrylate-co-methyl methacrylate) hydrogel tubes for use as nerve guidance channels. Biomaterials 2002;23:3843–3851. [PubMed: 12164188]

92. Dalton PD, Shoichet MS. Creating porous tubes by centrifugal forces for soft tissue application. Biomaterials 2001;22:2661–2669. [PubMed: 11519786]

93. Huang X, Unno H, Akehata T, Hirasa O. Analysis of Kinetic-Behavior of Temperature-Sensitive Water-Absorbing Hydrogel. Journal of Chemical Engineering of Japan 1987;20:123–128.

94. Kabra BG, Akhtar MK, Gehrke SH. Volume Change Kinetics of Temperature-Sensitive Poly(Vinyl Methyl-Ether) Gel. Polymer 1992;33:990–995.

95. Kabra BG, Gehrke SH. Synthesis of Fast Response, Temperature-Sensitive Poly(N-Isopropylacrylamide) Gel. Polymer Communications 1991;32:322–323.

96. Wu XS, Hoffman AS, Yager P. Synthesis and Characterization of Thermally Reversible Macroporous Poly(N-Isopropylacrylamide) Hydrogels. Journal of Polymer Science Part a-Polymer Chemistry 1992;30:2121–2129.

97. Yan Q, Hoffman AS. Synthesis of macroporous hydrogels with rapid swelling and deswelling properties for delivery of macromolecules. Polymer 1995;36:887–889.

98. Takehiko G, Yuko N, Shuji S. Novel synthesis of thermosensitive porous hydrogels. Journal of Applied Polymer Science 1998;69:895–906.

99. Lévesque SG, Lim RM, Shoichet MS. Macroporous interconnected dextran scaffolds of controlled porosity for tissue-engineering applications. Biomaterials 2005;26:7436–7446. [PubMed: 16023718]

100. Stenekes RJH, Franssen O, van Bommel EMG, Crommelin DJA, Hennink WE. The use of aqueous PEG/dextran phase separation for the preparation of dextran microspheres. International Journal of Pharmaceutics 1999;183:29–32. [PubMed: 10361149]

101. Righetti PG, Caglio S, Saracchi M, Quaroni S. Laterally Aggregated Polyacrylamide Gels for Electrophoresis. Electrophoresis 1992;13:587–595. [PubMed: 1459071]

102. Asnaghi D, Giglio M, Bossi A, Righetti PG. Large-scale microsegregation in polyacrylamide gels (spinodal gels). The Journal of Chemical Physics 1995;102:9736–9742.

103. Charlionet R, Levasseur L, Malandain JJ. Eliciting macroporosity in polyacrylamide and agarose gels with polyethylene glycol. Electrophoresis 1996;17:58–66. [PubMed: 8907519]

104. Righetti PG, Caglio S. On the Kinetics of Monomer Incorporation into Polyacrylamide Gels, as Investigated by Capillary Zone Electrophoresis. Electrophoresis 1993;14:573–582. [PubMed: 8375347]

105. Kwok AY, Prime EL, Qiao GG, Solomon DH. Synthetic hydrogels 2. Polymerization induced phase separation in acrylamide systems. Polymer 2003;44:7335–7344.

106. Kwok AY, Qiao GG, Solomon DH. Synthetic hydrogels. 1. Effects of solvent on poly(acrylamide) networks. Polymer 2003;44:6195–6203.

107. Kwok AY, Qiao GG, Solomon DH. Interpenetrating amphiphilic polymer networks of poly(2-hydroxyethyl methaerylate) and poly(ethylene oxide). Chemistry of Materials 2004;16:5650–5658.
108. Kwok AY, Qiao GG, Solomon DH. Synthetic hydrogels 3. Solvent effects on poly(2-hydroxyethyl methacrylate) networks. Polymer 2004;45:4017–4027.
109. Rembaum A, Yen SPS, Cheong E, Wallace S, Molday RS, Gordon IL, et al. Functional Polymeric Microspheres Based on 2-Hydroxyethyl Methacrylate for Immunochemical Studies. Macromolecules 1976;9:328–336. [PubMed: 944368]
110. Pelton RH, Chibante P. Preparation of aqueous latices with N-isopropylacrylamide. Colloids and Surfaces 1986;20:247–256.
111. Kawaguchi H, Fujimoto K, Mizuhara Y. Hydrogel microspheres III. Temperature-dependent adsorption of proteins on poly-N-isopropylacrylamide hydrogel microspheres. Colloid & Polymer Science 1992;270:53–57.
112. Leobandung W, Ichikawa H, Fukumori Y, Peppas NA. Monodisperse nanoparticles of poly(ethylene glycol) macromers and N-isopropyl acrylamide for biomedical applications. Journal of Applied Polymer Science 2003;87:1678–1684.
113. Kawaguchi H, Kawahara M, Yaguchi N, Hoshino F, Ohtsuka Y. Hydrogel Microspheres .1. Preparation of Monodisperse Hydrogel Microspheres of Sub-Micron or Micron Size. Polymer Journal 1988;20:903–909.
114. Kawaguchi H, Yamada Y, Kataoka S, Morita Y, Ohtsuka Y. Hydrogel Microspheres .2. Precipitation Copolymerization of Acrylamide with Comonomers to Prepare Monodisperse Hydrogel Microspheres. Polymer Journal 1991;23:955–962.
115. Hachisu S, Kobayashi Y, Kose A. Phase separation in monodisperse latexes. Journal of Colloid and Interface Science 1973;42:342–348.
116. Weissman JM, Sunkara HB, Tse AS, Asher SA. Thermally switchable periodicities and diffraction from mesoscopically ordered materials. Science 1996;274:959–960. [PubMed: 8875932]
117. Hellweg T, Dewhurst CD, Bruckner E, Kratz K, Eimer W. Colloidal crystals made of poly(N-isopropylacrylamide) microgel particles. Colloid and Polymer Science 2000;278:972–978.
118. Debord JD, Lyon LA. Thermoresponsive photonic crystals. Journal of Physical Chemistry B 2000;104:6327–6331.
119. Debord SB, Lyon LA. Influence of particle volume fraction on packing in responsive hydrogel colloidal crystals. Journal of Physical Chemistry B 2003;107:2927–2932.
120. Jones CD, Serpe MJ, Schroeder L, Lyon LA. Microlens formation in microgel/gold colloid composite materials via photothermal patterning. Journal of the American Chemical Society 2003;125:5292–5293. [PubMed: 12720438]
121. Nayak S, Debord SB, Lyon LA. Investigations into the deswelling dynamics and thermodynamics of thermoresponsive microgel composite films. Langmuir 2003;19:7374–7379.
122. Lyon LA, Debord JD, Debord SB, Jones CD, McGrath JG, Serpe MJ. Microgel colloidal crystals. Journal of Physical Chemistry B 2004;108:19099–19108.
123. Hu Z, Lu X, Gao J, Wang C. Polymer Gel Nanoparticle Networks. Advanced Materials 2000;12:1173–1176.
124. Hu Z, Lu X, Gao J. Hydrogel Opals. Advanced Materials 2001;13:1708–1712.
125. Huang G, Gao J, Hu Z, St. John JV, Ponder BC, Moro D. Controlled drug release from hydrogel nanoparticle networks. Journal of Controlled Release 2004;94:303–311. [PubMed: 14744482]
126. Cai T, Marquez M, Hu Z. Monodisperse Thermoresponsive Microgels of Poly(ethylene glycol) Analogue-Based Biopolymers. Langmuir 2007;23:8663–8666. [PubMed: 17658862]
127. Moro, DG.; St. John, JV.; Shannon, KF.; Ponder, BC., inventors. Method of Formation of Shape-Retentive Aggregates of Gel Particles and their Uses patent US patent application 20080063716. 2007.
128. Cai W, Gupta RB. Fast-responding bulk hydrogels with microstructure. Journal of Applied Polymer Science 2002;83:169–178.
129. Cho EC, Kim J-W, Fernandez-Nieves A, Weitz DA. Highly Responsive Hydrogel Scaffolds Formed by Three-Dimensional Organization of Microgel Nanoparticles. Nano Letters 2007;8:168–172. [PubMed: 18085810]

130. Cho EC, Kim J-W, Hyun DC, Jeong U, Weitz DA. Regulating Volume Transitions of Highly Responsive Hydrogel Scaffolds by Adjusting the Network Properties of Microgel Building Block Colloids. Langmuir 26:3854–3859. [PubMed: 20166725]
131. Shah RK, Kim J-W, Weitz DA. Monodisperse Stimuli-Responsive Colloidosomes by Self-Assembly of Microgels in Droplets. Langmuir 2009;26:1561–1565. [PubMed: 19950936]
132. Wu JJ, Shek PN. Synthesis and characterization of a novel in situ forming gel based on hydrogel dispersions. Journal of Biomedical Materials Research Part B: Applied Biomaterials 2009;90B: 738–744.
133. Suzuki D, Tsuji S, Kawaguchi H. Janus Microgels Prepared by Surfactant-Free Pickering Emulsion-Based Modification and Their Self-Assembly. Journal of the American Chemical Society 2007;129:8088–8089. [PubMed: 17552529]
134. Eichenbaum GM, Kiser PF, Simon SA, Needham D. pH and Ion-Triggered Volume Response of Anionic Hydrogel Microspheres. Macromolecules 1998;31:5084–5093. [PubMed: 9680449]
135. Kiser PF, Wilson G, Needham D. A synthetic mimic of the secretory granule for drug delivery. Nature 1998;394:459–462. [PubMed: 9697768]
136. Kiser PF, Wilson G, Needham D. Lipid-coated microgels for the triggered release of doxorubicin. J Control Release 2000;68:9–22. [PubMed: 10884575]
137. Gorelikov I, Field LM, Kumacheva E. Hybrid Microgels Photoresponsive in the Near-Infrared Spectral Range. Journal of the American Chemical Society 2004;126:15938–15939. [PubMed: 15584708]
138. Das M, Sanson N, Fava D, Kumacheva E. Microgels Loaded with Gold Nanorods:â€‰ Photothermally Triggered Volume Transitions under Physiological Conditionsâ€. Langmuir 2006;23:196–201. [PubMed: 17190504]
139. Hoare T, Pelton R. Charge-Switching, Amphoteric Glucose-Responsive Microgels with Physiological Swelling Activity. Biomacromolecules 2008;9:733–740. [PubMed: 18198833]
140. Banerjee P, Irvine DJ, Mayes AM, Griffith LG. Polymer latexes for cell-resistant and cell-interactive surfaces. Journal of Biomedical Materials Research 2000;50:331–339. [PubMed: 10737874]
141. Serpe MJ, Yarmey KA, Nolan CM, Lyon LA. Doxorubicin uptake and release from microgel thin films. Biomacromolecules 2005;6:408–413. [PubMed: 15638546]
142. Nolan CM, Serpe MJ, Lyon LA. Pulsatile release of insulin from Layer-by-Layer assembled microgel thin films. Macromolecular Symposia 2005;227:285–294.
143. Gan DJ, Lyon LA. Synthesis and protein adsorption resistance of PEG-modified poly(N-isopropylacrylamide) core/shell microgels. Macromolecules 2002;35:9634–9639.
144. Nolan CM, Reyes CD, Debord JD, Garcia AJ, Lyon LA. Phase transition behavior, protein adsorption, and cell adhesion resistance of poly(ethylene glycol) cross-linked microgel particles. Biomacromolecules 2005;6:2032–2039. [PubMed: 16004442]
145. Singh N, Bridges AW, Garcia AJ, Lyon LA. Covalent tethering of functional microgel films onto poly(ethylene terephthalate) surfaces. Biomacromolecules 2007;8:3271–3275. [PubMed: 17877399]
146. Bridges AW, Singh N, Burns KL, Babensee JE, Lyon LA, Garcia AJ. Reduced acute inflammatory responses to microgel conformal coatings. Biomaterials 2008;29:4605–4615. [PubMed: 18804859]
147. Lyon LA, Meng ZY, Singh N, Sorrell CD, John AS. Thermoresponsive microgel-based materials. Chemical Society Reviews 2009;38:865–874. [PubMed: 19421566]
148. Flodin P. The Sephadex story. Polymer Engineering & Science 1998;38:1220–1228.
149. Flodin, P. Dextran gels and their applications in gel filtration. Uppsala: Pharmacia; 1963.
150. Flodin, P., inventor. Process for preparing hydrophilic copolymerization and product obtained thereby patent US. 3,208,994. 1965.
151. Edman P, Ekman B, Sjoholm I. Immobilization of proteins in microspheres of biodegradable polyacryldextran. Journal of pharmaceutical sciences 1980;69:838–842. [PubMed: 6156234]
152. Reis CP, Neufeld RJ, Vilela S, Ribeiro AJ, Veiga F. Review and current status of emulsion/dispersion technology using an internal gelation process for the design of alginate particles. Journal of Microencapsulation 2006;23:245–257. [PubMed: 16801237]

153. Tanaka T, Sato E, Hirokawa Y, Hirotsu S, Peetermans J. Critical Kinetics of Volume Phase Transition of Gels. Physical Review Letters 1985;55:2455. [PubMed: 10032149]

154. Hirose Y, Amiya T, Hirokawa Y, Tanaka T. Phase transition of submicron gel beads. Macromolecules 1987;20:1342–1344.

155. Park TG, Hoffman AS. Effect of Temperature Cycling on the Activity and Productivity of Immobilized Beta-Galactosidase in a Thermally Reversible Hydrogel Bead Reactor. Applied Biochemistry and Biotechnology 1988;19:1–9. [PubMed: 3144242]

156. Drummond RK, Klier J, Alameda JA, Peppas NA. Preparation of poly(methacrylic acid-g-ethylene oxide) microspheres. Macromolecules 1989;22:3816–3818.

157. Meldal M. Pega: a flow stable polyethylene glycol dimethyl acrylamide copolymer for solid phase synthesis. Tetrahedron Letters 1992;33:3077–3080.

158. Gavelin, P.; Pehr-Rehnberg, NP.; Johannsen, I., inventors. Beaded and Cross-Linked Poly (Aminoalkylene)Matrix and Uses Thereof patent US Patent Application 2009/0023606A1. 2009.

159. Thornton PD, Mart RJ, Ulijn RV. Enzyme-responsive polymer hydrogel particles for controlled release. Advanced Materials 2007;19 1252-+.

160. Thornton PD, Mart RJ, Webb SJ, Ulijn RV. Enzyme-responsive hydrogel particles for the controlled release of proteins: designing peptide actuators to match payload. Soft Matter 2008;4:821–827.

161. Thornton PD, McConnell G, Ulijn RV. Enzyme responsive polymer hydrogel beads. Chemical Communications 2005:5913–5915. [PubMed: 16317473]

162. Kim J, Yaszemski MJ, Lu L. Three-dimensional porous biodegradable polymeric scaffolds fabricated with biodegradable hydrogel porogens. Tissue Eng Part C Methods 2009;15:583–594. [PubMed: 19216632]

163. Yun YH, Goetz DJ, Yellen P, Chen W. Hyaluronan microspheres for sustained gene delivery and site-specific targeting. Biomaterials 2004;25:147–157. [PubMed: 14580918]

164. Jia X, Yeo Y, Clifton RJ, Jiao T, Kohane DS, Kobler JB, et al. Hyaluronic Acid-Based Microgels and Microgel Networks for Vocal Fold Regeneration. Biomacromolecules 2006;7:3336–3344. [PubMed: 17154461]

165. Jha AK, Yang W, Kirn-Safran CB, Farach-Carson MC, Jia X. Perlecan domain I-conjugated, hyaluronic acid-based hydrogel particles for enhanced chondrogenic differentiation via BMP-2 release. Biomaterials 2009;30:6964–6975. [PubMed: 19775743]

166. Morimoto K, Katsumata H, Yabuta T, Iwanaga K, Kakemi M, Tabata Y, et al. Gelatin microspheres as a pulmonary delivery system: Evaluation of salmon calcitonin absorption. Journal of Pharmacy and Pharmacology 2000;52:611–617. [PubMed: 10875536]

167. Hong L, Tabata Y, Miyamoto S, Yamada K, Aoyama I, Tamura M, et al. Promoted bone healing at a rabbit skull gap between autologous bone fragment and the surrounding intact bone with biodegradable microspheres containing transforming growth factor-beta 1. Tissue Engineering 2000;6:331–340. [PubMed: 10992430]

168. Park H, Temenoff JS, Holland TA, Tabata Y, Mikos AG. Delivery of TGF-beta1 and chondrocytes via injectable, biodegradable hydrogels for cartilage tissue engineering applications. Biomaterials 2005;26:7095–7103. [PubMed: 16023196]

169. Holland TA, Tessmar JK, Tabata Y, Mikos AG. Transforming growth factor-beta 1 release from oligo(poly(ethylene glycol) fumarate) hydrogels in conditions that model the cartilage wound healing environment. J Control Release 2004;94:101–114. [PubMed: 14684275]

170. Tabata Y, Hijikata S, Muniruzzaman M, Ikada Y. Neovascularization effect of biodegradable gelatin microspheres incorporating basic fibroblast growth factor. Journal of Biomaterials Science-Polymer Edition 1999;10:79–94. [PubMed: 10091924]

171. Park H, Guo X, Temenoff JS, Tabata Y, Caplan AI, Kasper FK, et al. Effect of Swelling Ratio of Injectable Hydrogel Composites on Chondrogenic Differentiation of Encapsulated Rabbit Marrow Mesenchymal Stem Cells In Vitro. Biomacromolecules 2009;10:541–546. [PubMed: 19173557]

172. Guo X, Park H, Liu GP, Liu W, Cao YL, Tabata Y, et al. In vitro generation of an osteochondral construct using injectable hydrogel composites encapsulating rabbit marrow mesenchymal stem cells. Biomaterials 2009;30:2741–2752. [PubMed: 19232711]

173. Park H, Temenoff JS, Tabata Y, Caplan AI, Mikos AG. Injectable biodegradable hydrogel composites for rabbit marrow mesenchymal stem cell and growth factor delivery for cartilage tissue engineering. Biomaterials 2007;28:3217–3227. [PubMed: 17445882]

174. Nilsson K, Mosbach K. Preparation of immobilized animal cells. FEBS letters 1980;118:145–150. [PubMed: 7409188]

175. Nilsson K, Buzsaky F, Mosbach K. Growth of Anchorage-Dependent Cells on Macroporous Microcarriers. Bio-Technology 1986;4:989–990.

176. Green, BK.; Schleicher, L., inventors. Manifold record material patent US. 2,730,456. 1956.

177. Green, BK.; Schleicher, L., inventors. Pressure responsive record materials patent US. 2,730,457. 1956.

178. Green, BK., inventor. Oil-containing microscopic capsules and method of making them patent US. 2,800,458. 1957.

179. Phares RE Jr, Sperandio GJ. Coating Pharmaceuticals by Coacervation. Journal of pharmaceutical sciences 1964;53:515–518. [PubMed: 14193883]

180. Jizomoto H. Phase-Separation Induced in Gelatin Base Coacervation Systems by Addition of Water-Soluble Nonionic Polymers-I - Microencapsulation. Journal of pharmaceutical sciences 1984;73:879–882. [PubMed: 6470947]

181. Jizomoto H. Phase-Separation Induced in Gelatin Base Coacervation Systems by Addition of Water-Soluble Nonionic Polymers .2. Effect of Molecular-Weight. Journal of pharmaceutical sciences 1985;74:469–472. [PubMed: 3999011]

182. Yin X, Stover HDH. Hydrogel Microspheres by Thermally Induced Coacervation of Poly(N,N-dimethylacrylamide-co-glycidyl methacrylate) Aqueous Solutions. Macromolecules 2003;36:9817–9822.

183. Yin XC, Stover HDH. Temperature-sensitive hydrogel microspheres formed by liquid-liquid phase transitions of aqueous solutions of poly(N,N-dimethylacrylamide-co-allyl methacrylate). Journal of Polymer Science Part a-Polymer Chemistry 2005;43:1641–1648.

184. Yin XC, Stover DH. Hydrogel microspheres formed by complex coacervation of partially MPEG-grafted poly(styrene-alt-maleic anhydride) with PDADMAC and cross-linking with polyamines. Macromolecules 2003;36:8773–8779.

185. Jain S, Yap WT, Irvine DJ. Synthesis of Protein-Loaded Hydrogel Particles in an Aqueous Two-Phase System for Coincident Antigen and CpG Oligonucleotide Delivery to Antigen-Presenting Cells. Biomacromolecules 2005;6:2590–2600. [PubMed: 16153096]

186. Martin Y, Vermette P. Low-fouling amine-terminated poly(ethylene glycol) thin layers and effect of immobilization conditions on their mechanical and physicochemical properties. Macromolecules 2006;39:8083–8091.

187. Stenekes RJH, Franssen O, van Bommel EMG, Crommelin DJA, Hennink WE. The Preparation of Dextran Microspheres in an All-Aqueous System: Effect of the Formulation Parameters on Particle Characteristics. Pharmaceutical Research 1998;15:557–561. [PubMed: 9587951]

188. Franssen O, Hennink WE. A novel preparation method for polymeric microparticles without the use of organic solvents. International Journal of Pharmaceutics 1998;168:1–7.

189. Stenekes RJH, Franssen O, van Bommel EMG, Crommelin DJA, Hennink WE. The use of aqueous PEG dextran phase separation for the preparation of dextran microspheres. International Journal of Pharmaceutics 1999;183:29–32. [PubMed: 10361149]

190. Franssen O, Vandervennet L, Roders P, Hennink WE. Degradable dextran hydrogels: controlled release of a model protein from cylinders and microspheres. Journal of Controlled Release 1999;60:211–221. [PubMed: 10425327]

191. De Groot CJ, Cadee JA, Koten JW, Hennink WE, Den Otter W. Therapeutic efficacy of IL-2-loaded hydrogels in a mouse tumor model. International Journal of Cancer 2002;98:134–140.

192. Stenekes R, Loebis A, Fernandes C, Crommelin D, Hennink W. Controlled Release of Liposomes from Biodegradable Dextran Microspheres: A Novel Delivery Concept. Pharmaceutical Research 2000;17:664–669. [PubMed: 10955838]

193. Van Tomme SR, van Steenbergen MJ, De Smedt SC, van Nostrum CF, Hennink WE. Self-gelling hydrogels based on oppositely charged dextran microspheres. Biomaterials 2005;26:2129–2135. [PubMed: 15576188]

194. Van Tomme SR, De Geest BG, Braeckmans K, De Smedt SC, Siepmann F, Siepmann J, et al. Mobility of model proteins in hydrogels composed of oppositely charged dextran microspheres studied by protein release and fluorescence recovery after photobleaching. Journal of Controlled Release 2005;110:67–78. [PubMed: 16253375]

195. Van Tomme SR, van Nostrum CF, de Smedt SC, Hennink WE. Degradation behavior of dextran hydrogels composed of positively and negatively charged microspheres. Biomaterials 2006;27:4141–4148. [PubMed: 16600367]

196. Van Tomme SR, van Nostrum CF, Dijkstra M, De Smedt SC, Hennink WE. Effect of particle size and charge on the network properties of microsphere-based hydrogels. European Journal of Pharmaceutics and Biopharmaceutics 2008;70:522–530. [PubMed: 18582574]

197. Van Tomme SR, Mens A, van Nostrum CF, Hennink WE. Macroscopic Hydrogels by Self-Assembly of Oligolactate-Grafted Dextran Microspheres. Biomacromolecules 2008;9:158–165. [PubMed: 18081253]

198. De Geest BG, Stubbe BG, Jonas AM, Van Thienen T, Hinrichs WL, Demeester J, et al. Self-exploding lipid-coated microgels. Biomacromolecules 2006;7:373–379. [PubMed: 16398538]

199. De Geest BG, De Koker S, Immesoete K, Demeester J, De Smedt SC, Hennink WE. Self-Exploding Beads Releasing Microcarriers. Advanced Materials 2008;20 3687-+.

200. De Geest BG, McShane MJ, Demeester J, De Smedt SC, Hennink WE. Microcapsules Ejecting Nanosized Species into the Environment. Journal of the American Chemical Society 2008;130:14480–14482. [PubMed: 18847265]

201. Van Thienen TG, Demeester J, De Smedt SC. Screening poly(ethyleneglycol) micro- and nanogels for drug delivery purposes. Int J Pharm 2008;351:174–185. [PubMed: 18061378]

202. Zhang XZ, Chu CC. A responsive poly(N-isopropylacrylamide)/poly(ethylene glycol) diacrylate hydrogel microsphere. Colloid and Polymer Science 2004;282:1415–1420.

203. Zhang XZ, Chu CC. Fabrication and characterization of microgel-impregnated, thermosensitive PNIPAAm hydrogels. Polymer 2005;46:9664–9673.

204. Baker, RW. Membrane Technology and Applications. New York: McGraw-Hill; 2000.

205. Mulder, J. Basic principles of membrane technology. Dordrecht: Kluwer; 1996.

206. Strathmann H, Scheible P, Baker RW. A rationale for the preparation of Loeb–Sourirajan-type cellulose acetate membranes. J Appl Polym Sci 1971;15:811–828.

207. Weigel T, Schinkel G, Lendlein A. Design and preparation of polymeric scaffolds for tissue engineering. Expert Review of Medical Devices 2006;3:835–851. [PubMed: 17280547]

208. Katz, MG.; Wydeven, T. Poly(vinyl alcohol) membranes for reverse osmosis. In: Turbak, AF., editor. Synthetic Membranes, ACS Symposium Series. Vol. Vol 153. Washington, D.C.: American Chemical Society; 1981. p. 383-398.

209. Peter S, Hese N, Stefan R. Phenol-selective, highly resistant ro-membranes made from pva for purification of toxic industrial-wastes. Desalination 1976;19:161–167.

210. Chang HN. Reverse-osmosis separation of inorganic salts using polyvinylalcohol membranes. Desalination 1982;42:63–77.

211. Brannon ML, Peppas NA. Solute diffusion in swollen membranes.8. Characterization of and diffusion in asymmetric membranes. J Membr Sci 1987;32:125–138.

212. Crooks CA, Douglas JA, Broughton RL, Sefton MV. Microencapsulation of mammalian-cells in a hema-mma copolymer - effects on capsule morphology and permeability. Journal of biomedical materials research 1990;24:1241–1262. [PubMed: 2211747]

213. Hwang JR, Sefton MV. The effects of polymer concentration and a pore-forming agent (PVP) on HEMA-MMA microcapsule structure and permeability. J Membr Sci 1995;108:257–268.

214. Honiger J, Balladur P, Mariani P, Calmus Y, Vaubourdolle M, Delelo R, et al. Permeability and biocompatibility of a new hydrogel used for encapsulation of hepatocytes. Biomaterials 1995;16:753–759. [PubMed: 7492705]

215. Maury F, Honiger J, Pelaprat D, Baudrimont M, Borderie V, Rostene W, et al. In-vitro development of corneal epithelial cells on a new hydrogel for epikeratoplasty. J Mater Sci-Mater Med 1997;8:571–576. [PubMed: 15348709]

216. Tromp RH, Rennie AR, Jones RAL. Kinetics of the Simultaneous Phase-Separation and Gelation in Solutions of Dextran and Gelatin. Macromolecules 1995;28:4129–4138.

217. Beginn U, Fischer E, Pieper T, Mellinger F, Kimmich R, Moller M. Controlled preparation of nanometer-sized supramolecular cylinders of poly(ethylene oxide) embedded in methacrylate matrices. Journal of Polymer Science Part a-Polymer Chemistry 2000;38:2041–2056.

218. Fischer E, Beginn U, Fatkullin N, Kimmich R. Nanoscopic poly(ethylene oxide) strands embedded in semi-interpenetrating methacrylate networks. Preparation method and quantitative characterization by field-gradient NMR diffusometry. Macromolecules 2004;37:3277–3286.

219. Benton JA, DeForest CA, Vivekanandan V, Anseth KS. Photocrosslinking of gelatin macromers to synthesize porous hydrogels that promote valvular interstitial cell function. Tissue Eng Part A 2009;15:3221–3230. [PubMed: 19374488]

220. Kim SH, Chu CC. Synthesis and characterization of dextran-methacrylate hydrogels and structural study by SEM. Journal of biomedical materials research 1999;49:517–527. [PubMed: 10602085]

221. Kim SH, Chu CC. Pore structure analysis of swollen dextran-methacrylate hydrogels by SEM and mercury intrusion porosimetry. Journal of biomedical materials research 2000;53:258–266. [PubMed: 10813766]

222. Li Q, Williams CG, Sun DDN, Wang J, Leong K, Elisseeff JH. Photocrosslinkable polysaccharides based on chondroitin sulfate. Journal of Biomedical Materials Research Part A 2004;68A:28–33. [PubMed: 14661246]

223. Nichols MD, Scott EA, Elbert DL. Factors affecting size and swelling of poly(ethylene glycol) microspheres formed in aqueous sodium sulfate solutions without surfactants. Biomaterials 2009;30:5283–5291. [PubMed: 19615738]

224. Scott EA, Nichols MD, Willits RK, Elbert DL. Modular scaffolds assembled around living cells using poly(ethylene glycol) microspheres with macroporation via a non-cytotoxic porogen. Acta Biomaterialia 2009;6:29–38. [PubMed: 19607945]

225. Kriwet B, Walter E, Kissel T. Synthesis of bioadhesive poly(acrylic acid) nano- and microparticles using an inverse emulsion polymerization method for the entrapment of hydrophilic drug candidates. Journal of Controlled Release 1998;56:149–158. [PubMed: 9801438]

226. Candau, F. Inverse emulstion and microemulsion polymerization. In: Lovell, PA.; Elaasser, MS., editors. Emulsion polymerization and emulsion polymers. Chichester: John Wiley and Sons; 1997. p. 723-741.

227. Mouaziz H, Lacki K, Larsson A, Sherrington DC. Synthesis of porous microspheres via self-assembly of monodisperse polymer nanospheres. Journal of Materials Chemistry 2004;14:2421–2424.

228. Lally S, Bird R, Freemont TJ, Saunders BR. Microgels containing methacrylic acid: effects of composition on pH-triggered swelling and gelation behaviours. Colloid and Polymer Science 2009;287:335–343.

229. Lally S, Mackenzie P, LeMaitre CL, Freemont TJ, Saunders BR. Microgel particles containing methacrylic acid: pH-triggered swelling behaviour and potential for biomaterial application. Journal of Colloid and Interface Science 2007;316:367–375. [PubMed: 17765913]

230. Freemont TJ, Saunders BR. PH-responsive microgel dispersions for repairing damaged load-bearing soft tissue. Soft Matter 2008;4:919–924.

231. Vinogradov S, Batrakova E, Kabanov A. Poly(ethylene glycol)-polyethyleneimine NanoGel(TM) particles: novel drug delivery systems for antisense oligonucleotides. Colloids and Surfaces B: Biointerfaces 1999;16:291–304.

232. Vinogradov SV, Bronich TK, Kabanov AV. Nanosized cationic hydrogels for drug delivery: preparation, properties and interactions with cells. Advanced Drug Delivery Reviews 2002;54:135–147. [PubMed: 11755709]

233. Payne RG, McGonigle JS, Yaszemski MJ, Yasko AW, Mikos AG. Development of an injectable, in situ crosslinkable, degradable polymeric carrier for osteogenic cell populations. Part 2. Viability of encapsulated marrow stromal osteoblasts cultured on crosslinking poly(propylene fumarate). Biomaterials 2002;23:4373–4380. [PubMed: 12219827]

234. Payne RG, McGonigle JS, Yaszemski MJ, Yasko AW, Mikos AG. Development of an injectable, in situ crosslinkable, degradable polymeric carrier for osteogenic cell populations. Part 3.

Proliferation and differentiation of encapsulated marrow stromal osteoblasts cultured on crosslinking poly(propylene fumarate). Biomaterials 2002;23:4381–4387. [PubMed: 12219828]

235. Payne RG, Yaszemski MJ, Yasko AW, Mikos AG. Development of an injectable, in situ crosslinkable, degradable polymeric carrier for osteogenic cell populations. Part 1. Encapsulation of marrow stromal osteoblasts in surface crosslinked gelatin microparticles. Biomaterials 2002;23:4359–4371. [PubMed: 12219826]
236. Oh JK, Drumright R, Siegwart DJ, Matyjaszewski K. The development of microgels/nanogels for drug delivery applications. Progress in Polymer Science 2008;33:448–477.
237. Van Thienen TG, Lucas B, Demeester J, De Smedt SC. On the synthesis and characterization of biodegradable dextran nanogels with tunable degradation properties. J Control Release 2006;116:e12–e13. [PubMed: 17718944]
238. Van Thienen TG, Lucas B, Flesch FM, van Nostrum CF, Demeester J, De Smedt SC. On the synthesis and characterization of biodegradable dextran nanogels with tunable degradation properties. Macromolecules 2005;38:8503–8511.
239. Missirlis D, Hubbell JA, Tirelli N. Thermally-induced glass formation from hydrogel nanoparticles. Soft Matter 2006;2:1067–1075.
240. Missirlis D, Tirelli N, Hubbell JA. Amphiphilic hydrogel nanoparticles. Preparation, characterization, and preliminary assessment as new colloidal drug carriers. Langmuir 2005;21:2605–2613. [PubMed: 15752059]
241. Missirlis D, Kawamura R, Tirelli N, Hubbell JA. Doxorubicin encapsulation and diffusional release from stable, polymeric, hydrogel nanoparticles. European Journal of Pharmaceutical Sciences 2006;29:120–129. [PubMed: 16904301]
242. Yang Z, Ding J. A Thermosensitive and Biodegradable Physical Gel with Chemically Crosslinked Nanogels as the Building Block. Macromolecular Rapid Communications 2008;29:751–756.
243. Oh JK, Tang CB, Gao HF, Tsarevsky NV, Matyjaszewski K. Inverse miniemulsion ATRP: A new method for synthesis and functionalization of well-defined water-soluble/cross-linked polymeric particles. Journal of the American Chemical Society 2006;128:5578–5584. [PubMed: 16620132]
244. Anton N, Benoit JP, Saulnier P. Design and production of nanoparticles formulated from nanoemulsion templates-a review. J Control Release 2008;128:185–199. [PubMed: 18374443]
245. Anton N, Vandamme TF. The universality of low-energy nano-emulsification. International Journal of Pharmaceutics 2009;377:142–147. [PubMed: 19454306]
246. Yamamoto M, James D, Li H, Butler J, Rafii S, Rabbany S. Generation of stable co-cultures of vascular cells in a honeycomb alginate scaffold. Tissue engineering 2010;16:299–308. [PubMed: 19705957]
247. Despang F, Borner A, Dittrich R, Tomandl G, Pompe W, Gelinsky M. Alginate/calcium phosphate scaffolds with oriented, tube-like pores. Materialwissenschaft Und Werkstofftechnik 2005;36:761–767.
248. Dittrich R, Tomandl G, Despang F, Bernhardt A, Hanke T, Pompe W, et al. Scaffolds for hard tissue engineering by ionotropic gelation of alginate-influence of selected preparation parameters. Journal of the American Ceramic Society 2007;90:1703–1708.
249. Peppas NA, Stauffer SR. Reinforced Uncrosslinked Poly (Vinyl Alcohol) Gels Produced by Cyclic Freezing-Thawing Processes - a Short Review. Journal of Controlled Release 1991;16:305–310.

Glossary*

Polymerization types

Step growth polymerization	proceeds by a polycondensation or polyaddition in which reactions occur between chains of all sizes. Polycondensations use condensation reactions that produce a byproduct, such as water in the reaction of a carboxylic acid and amine. Polyadditions use addition reactions that do not produce a byproduct, such as the addition of a thiol to a vinyl group.

Chain growth polymerization	proceeds by a chain reaction, typically free radical-mediated but also including ring opening or ionic polymerizations, in which only monomers may add to a growing chain.
Emulsion polymerization	occurs with the monomer and initiator in different phases, and on average less than one radical per polymerization locus at a given time.
Suspension polymerization	occurs with the monomer and initiator in the same phase, and on average more than one radical per polymerization locus at a given time. Many of the hydrogel microsphere production techniques that are called ‘emulsion polymerizations’ are actually suspension polymerizations. Polycondensations or polyadditions are by necessity either suspension polymerizations or interfacial polymerizations.
Interfacial polymerization	is a condensation polymerization in which the reactants are soluble in different phases.
Miniemulsion polymerization	occurs with monomer suspended within a thermodynamically unstable but kinetically stable emulsion.
Microemulsion polymerization	occurs with monomer suspended within a thermodynamically stable emulsion.
Precipitation/ dispersion polymerization	occurs when the monomer is soluble in the continuous phase but the polymer is not.

Materials

Microgel	is a particle of gel of any shape with an equivalent diameter of approximately 0.1 to 100 μm (Ref. 32). Also has historically referred to large, highly crosslinked polymers present near the gel point during network formation, leading to potential confusion.
Nanogel	is a particle of gel of any shape with an equivalent diameter of approximately 1 to 100 nm (Ref. 32).
Macroporous	biomaterials have pore sizes greater than 1 μm.§
Microporous	biomaterials have pore sizes between 100 nm and 1 μm.§
Nanoporous	biomaterials have pore sizes less than 100 nm. § § New convention proposed here. See text for current definition.

Thermodynamics

Binodal line	defines compositions that have the same chemical potential and minimize the net free energy of mixing.
Spinodal line	defines compositions where $\partial^2 \Delta F_{mix} / \partial \varphi^2 = 0$.
Nucleation and growth	is a process that allows phase separation between the binodal and spinodal line, via a ternary component or phase that stabilizes concentration fluctuations.
Spinodal decomposition	is the spontaneous separation of phases after crossing the spinodal line.

Cloud point	is experimentally measured turbidity indicating phase separation. Assumed to be equivalent to the binodal point.
LCST	is a lower critical solution temperature that is associated with phase separation upon heating. This is the temperature at the critical point where the binodal and spinodal lines meet.
Phase separations	
χ-induced phase separation	is caused by a change in one of the variables that affect the Flory interaction parameter (χ), e.g. temperature or solvent composition.
Reaction-induced phase separation	is caused by an increase in molecular weight of one of the components of the reaction.
Thermally induced phase separation	is a specific type of χ-induced phase separation that may lead to unique phase morphologies due to the absence of mixing or solvent exchange.
Coarsening	is an increase in the average size of domains during phase separation, ultimately leading the formation of macroscopic layers. In the later stages of a phase separation, domain sizes increase by coalescence or Ostwald ripening.
Coalescence	is the merging of two droplets that come into close contact due to diffusion or convection.
Ostwald ripening	is the transfer of molecules through the continuous phase from smaller droplets with higher surface energy to larger droplets with lower surface energy.
Percolation-to-cluster transition	is transition in the morphology of phase separated domains accompanied by a change in the growth law. Initially following a thermally induced phase separation, the phases may exist in bicontinuous, percolated morphologies. Hydrodynamics dominate growth of the percolated domains, which follows a *diameter* ∝ *time* growth law. Diffusion dominates growth after the percolated phase breaks up into droplets (clusters). Growth in mean droplet size occurs by coalescence or Ostwald ripening, which both follow a *diameter* ∝ $time^{1/3}$ growth law.
Pinning	is a dramatic decrease in the rate of growth of phase separated domains, for example at the percolation-to-cluster transition, but may also occur due to vitrification, crystallization or gelation.
Gelation	
ν-induced syneresis	results in exudation of solvent from a gel due to an increase in the number of crosslinks (ν = *number of elastically active crosslinks in the gel*).
χ-induced syneresis	results in exudation of solvent from a gel due to a change in solvent-polymer interactions (χ = *Flory interaction parameter*), most likely is due to a change in solvent composition or temperature. Both ν-induced and χ-induced syneresis are directly predicted by the Flory-Rehner equation.

Microsyneresis	occurs when the solvent that should be exuded instead becomes trapped within the gel, usually as droplets. Note that none of these terms effectively describes gels that result from the aggregation of microparticles formed by a precipitation polymerization.
Colloids	
Simple coacervates	are two or more coexisting liquid-liquid phases, typically formed from single proteins or polysaccharides dissolved in water.
Complex coacervates	are two or more coexisting liquid-liquid phases that result due to electrostatic interactions between charged macromolecules.

* IUPAC definitions exist for most of these terms and can be found at http://goldbook.iupac.org. A brief description by the author is presented here unless otherwise noted.

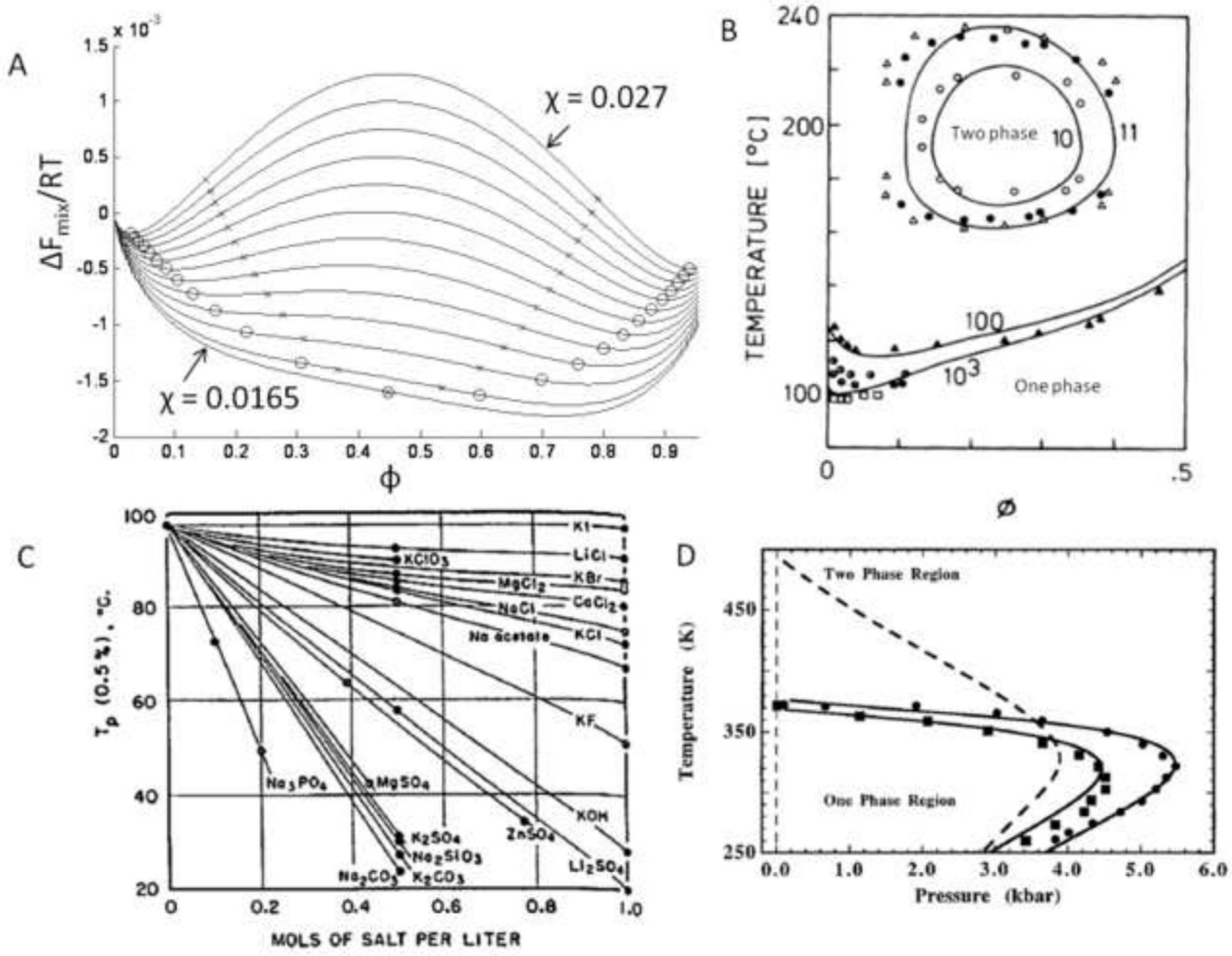

Figure 1. Thermodynamics of phase separation

(A) The Flory-Huggins equation (Equation [1]) describes the free energy of mixing as a function of composition (ϕ). The free energy of mixing is shown for a mixture of two polymers (degrees of polymerization of 150 and 100) and different values of the Flory interaction parameter (χ). Binodal points are shown as open circles and spinodal points are shown as x's. The dependence of the Flory interaction parameter on temperature determines if a lower or upper critical solution temperature exists. The critical point occurs at χ = 0.0165. (B) Phase diagram of PEG in water. The degree of polymerization of PEG is listed next to each binodal line. A one phase solution exists below the binodal lines, with the minima of the lines at the critical temperature (lower critical solution temperature, LCST). For low molecular weight PEG, closed loop behavior is observed, with an upper critical solution temperature (UCST) above the LCST. Adapted from Matsuyama & Tanaka, *Physical Review Letters*, 65, 341–344, 1990. (C) Salts greatly affect the LCST of PEG in water. Kosmotropic (water-structuring) salts are most effective at reducing the LCST. From Bailey & Callard, *J. Appl. Polym. Sci.*, 1, 56–62, 1959. (D) Pressure also affects the phase behavior. Phase separation occurs at room temperature for PEG mol. wt. 21,000 (circles), PEG mol. wt. 1360 (squares) and PVP (dotted line) in water at elevated pressures. Adapted with permission from Sun & King, *Macromolecules*, 31, 6383–6386, Copyright 1998 American Chemical Society.

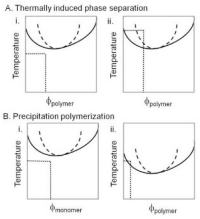

Figure 2. Hypothetical phase diagrams for a polymer exhibiting LCST phase behavior

(A) In a thermally induced phase separation, the solution is initially a single phase (i). The temperature is raised until the two phase region is entered (ii). The binodal line is solid and the spinodal line is dashed. If the solution is 'quenched' deeply so as to cross the spinodal line, phase separation is by spinodal decomposition. (B) In a precipitation polymerization, the temperature remains constant. The monomer is soluble throughout the polymerization (i). The polymer that forms has a different phase diagram from the monomer (ii). Polymer chains with different degrees of polymerization have distinct phase diagrams, as evident from the Flory-Huggins equation (Equation [1]). At the polymerization temperature, polymer chains above a certain degree of polymerization and concentration may phase separate. As shown in (ii), phase separation would be by nucleation and growth because only the binodal line is surpassed, while phase separation by spinodal decomposition will occur in (i).

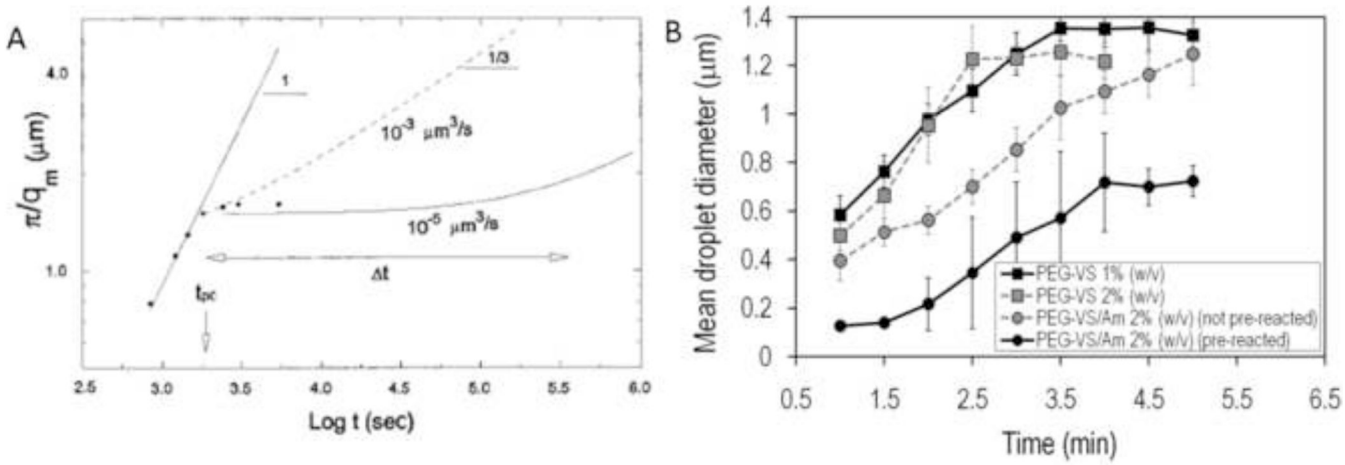

Figure 3. 'Pinning' of phase separation during spinodal decomposition

(A) The inverse of the wave vector with peak intensity, q_m, reveals the characteristic dimension of the phase separated domains. This is measured over time following a deep quench beyond the spinodal point of a poly(butadiene)/poly(isoprene) blend. The log-log plot reveals the power law nature of the process. Initially, the slope of one indicates a linear relationship between the characteristic size of the phase separated domain and time. Eventually, the power law exponent changes and growth appears to halt (i.e. 'pinned'). In fact, the growth law has simply changed, with an exponent at longer times of 1/3. The change in growth law occurs at the percolation-to-cluster transition. Reprinted with permission from Crist, B., *Macromolecules*, 29, 7276–7279, Copyright 1996 American Chemical Society. (B) The same phenomenon can be observed with PEG in PBS + 0.6 M sodium sulfate. When the temperature is raised to 37°C, dynamic light scattering showed a linear growth in the mean diameter, followed by pinning. This occurred with PEG alone at 1% or 2% (w/w), or with solutions of reactive PEGs. The reactive PEGs were either mixed immediately prior to phase separation or allowed to react for about 6 h prior to phase separation ('pre-reacted'). Reprinted from *Biomaterials*, 30, Nichols et al., "Factors affecting size and swelling of poly(ethylene glycol) microspheres formed in aqueous sodium sulfate solutions without surfactants", 5283–5291, Copyright 2009 with permission from Elsevier.

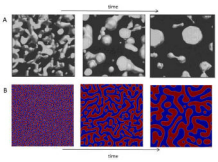

Figure 4. Spinodal decomposition and the percolation-to-cluster transition

(A) Direct visualization of the percolation-to-cluster transition by scanning confocal microscopy (the ‘clusters’ are the spherical domains). Fluorescently labeled poly(butadiene) was phase separated from poly(styrene-*ran*-butadiene) by spinodal decomposition following a deep quench. Reprinted with permission from Takeno et al., *Macromolecules*, 33, 9657–9665, Copyright 2000 American Chemical Society. (B) Solution to the Cahn-Hilliard equation that describes phase separation by spinodal decomposition and coarsening by Ostwald ripening. At the first time point, both red and blue phases percolate the entire area and exist as a bicontinuous network. Over time, the larger domains grow by absorbing mass from the smaller domains, with surface area minimized by adopting more spherical morphologies.

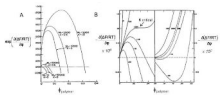

Figure 5. Gelation is a form of phase separation

(A) The chemical potential of a gel as a function of the polymer volume fraction determines the degree of swelling in excess solvent. No polymer exists outside the gel, so the equilibrium volume fractions of the fully swelled gel must fall on the dotted line (where the chemical potential is zero). M_c is the molecular weight between crosslinks; as M_c decreases from 50,000 to 5000 at constant K, the number of crosslinks (ν) in the gel increases and the equilibrium amount of polymer in the gel (ϕ) increases (i.e. the gel deswells). Decreased swelling with decreasing M_c is ν-*induced syneresis*. K contains the Flory interaction parameter (χ); as K increases at constant M_c, the interaction between solvent and monomer subunits becomes less favorable. Decreased swelling with increasing K is χ-*induced syneresis*. Reprinted with permission and adapted from Flory, P.J. & Rehner, J., "Statistical Mechanics of Cross-Linked Polymer Networks II. Swelling", *J. Chem. Phys.*, 11, 521–526, Copyright 1943, American Institute of Physics. (B) For comparison, the chemical potential for a polymer in solution as described by the Flory-Huggins equation (first derivative of equation [1] with respect to composition). The composition of the first phase will be to the left of the maximum, while the composition of the second phase will be to the right of the minimum (note that the two sides of the plot are on different scales). The numbers next to each curve are values of K. The arrow points to the critical value of K for phase separation. The chemical potential of the phase separated solutions is not necessarily zero but will be some value between the maximum and minimum that minimizes the total free energy of the solution (which is not apparent from this diagram alone). The figure illustrates the basis of χ-*induced phase separation*, but does not show the effects of increasing the degree of polymerization (N_A in equation [1]), which causes *reaction-induced phase separation*. Reprinted with permission and adapted from Flory, P.J., "Thermodynamics of High Polymer Solutions", *J. Chem. Phys.*, 10, 51–61, copyright 1942, American Institute of Physics.

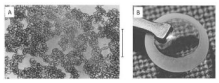

Figure 6. Porous HEMA hydrogels formed under conditions that promote precipitation polymerization

(A) Sponge-like poly(HEMA) gel formed in the presence of high concentrations of water. Note that the gel consists of microparticles with a narrow size distribution. This appears to be the result of coalescence of microparticles that formed by precipitation polymerization. Scale bar is 100 μm. Reprinted from Barvic et al., *J. Biomed. Mater. Res.*, 1, 313–323, 1967. (B) A poly (HEMA) corneal replacement device. An optically clear center region is formed using a low concentration of water and a macroporous skirt is formed using a high concentration of water. The macroporous region is designed to allow tissue ingrowth for better integration of the device. Reprinted by permission from Macmillan Publishers Ltd: *Eye*, 17, Hicks et al., 385–392, copyright 2003.

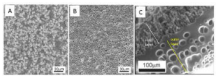

Figure 7. The mode of polymerization depends on subtle differences in reaction conditions

(A) A ‘macroporous’ poly(HEMA) hydrogel crosslinked with greater than 80% water showed the beaded morphology consistent with the coalescence of microparticles formed under precipitation polymerization conditions. (B) A ‘microporous’ poly(HEMA) hydrogel crosslinked with a lower water concentration than (A) but with more water than the equilibrium water concentration of the fully swollen hydrogel. The micropores may have formed by ν-induced microsyneresis. (C) Tube of hydrogel formed by spinning the polymerizing solution. HEMA was mixed with methyl methacrylate, water and a crosslinker. The inner region had a beaded morphology. The outer region was a nearly homogenous gel surrounding large pores. The outer region may have completely phase separated prior to gelation, while the inner layer resulted from a precipitation polymerization. Reprinted from *Biomaterials*, 23, Dalton et al., “Manufacture of poly(2-hydroxyethyl methacrylate-co-methyl methacrylate) hydrogel tubes for use as nerve guidance channels”, 3843–3851, Copyright 2002, with permission from Elsevier.

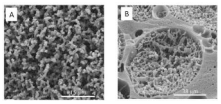

Figure 8. The mode of polymerization depends on subtle differences in reaction conditions

(A) Dextran-methacrylate (dextran-MA) was crosslinked in the presence of PEG. Within a narrow range of PEG concentrations, the dextran-MA was soluble, but became insoluble upon polymerization. A precipitation polymerization thus may have produced the beaded morphology. (B) At higher concentrations of dextran-MA, the PEG and dextran-MA may have phase separated before polymerization. The dextran-MA-rich phase produced a continuous hydrogel containing large pores. Inside the large pores, a precipitation polymerization may have occurred in the PEG-rich phase. This was likely due to the presence of some amount of dextran-MA within the PEG-rich phase at equilibrium. Reprinted and adapted from *Biomaterials*, 26, Levesque et al., "Macroporous interconnected dextran scaffolds of controlled porosity for tissue-engineering applications", 7436–7446, Copyright 2005, with permission from Elsevier.

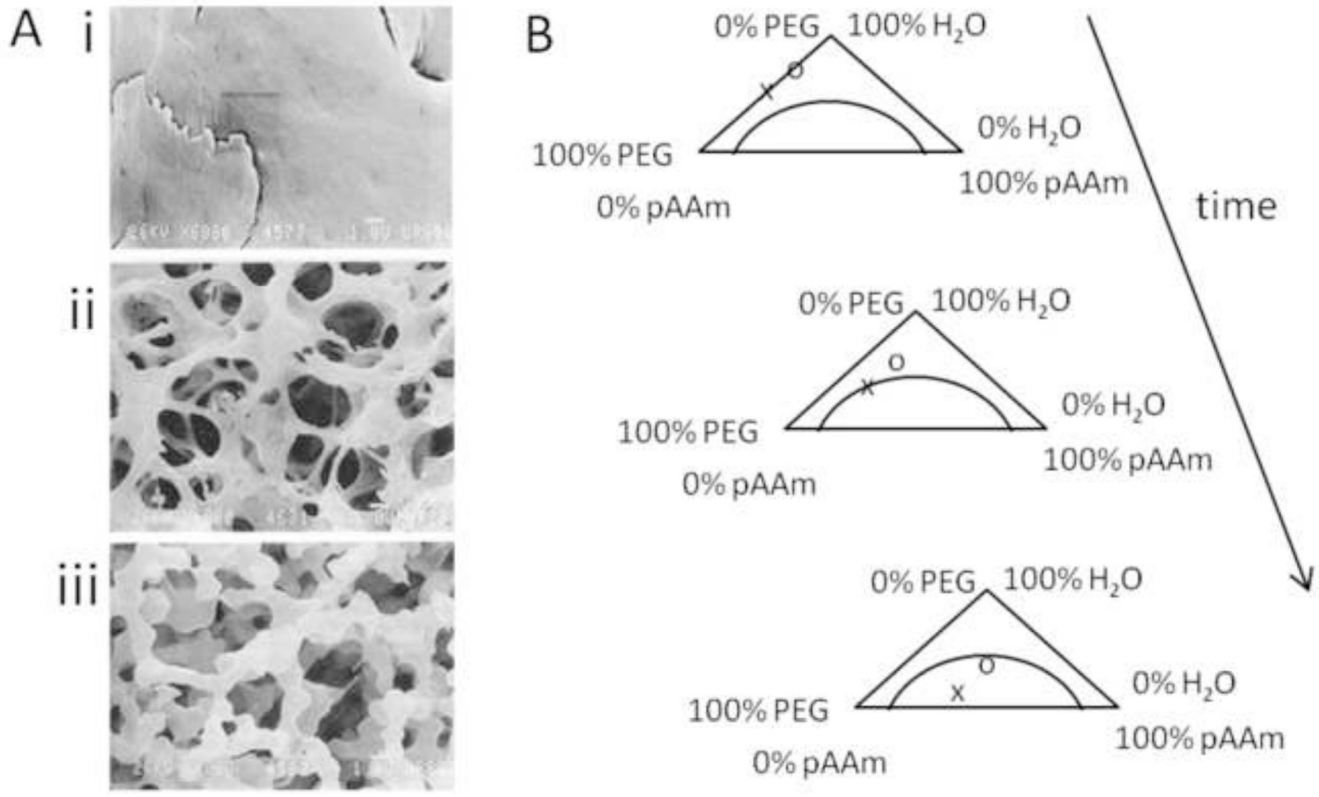

Figure 9. Polyacrylamide gels are macroporous if polymerized in the presence of PEG

(A) Poly(acrylamide) gel polymerized with (i) 0% PEG, (ii) 2.5% PEG, (iii) 5% PEG. Reprinted from Charlionet et al, "Eliciting macroporosity in polyacrylamide and agarose gels with polyethylene glycol", *Electrophoresis*, 1996, 17, 58–66. Copyright Wiley-VCH Verlag GmbH & Co. KGaA. Reproduced with permission. (B) A hypothetical ternary phase diagram for poly(acrylamide) (pAAm), PEG and water to explain the increase in pore size with higher PEG concentrations. At the start of the reaction, no poly(acrylamide) is present. PEG is present at a higher (x) or lower concentration (o). As the poly(acrylamide) concentration increases, the higher concentration PEG solution phase separates first. This results in larger pores due to increased time for phase separation. Redrawn based on Asnaghi et al., *J. Chem. Phys.* 102, 9736–9742, 1995.

Figure 10. Near monodisperse microspheres by precipitation polymerization

(A) Poly(HEMA) microspheres formed by gamma-irradiation of HEMA and BIS at a monomer concentration of 5% in water. Reprinted with permission from *Macromolecules*, 9, Rembaum et al., "Functional Polymeric Microspheres Based on 2-Hydroxyethyl Methacrylate for Immunochemical Studies", 328–336, Copyright 1976 American Chemical Society. (B) Poly (NIPAAm) microspheres. Reprinted from *Colloids and Surfaces*, 20, Pelton & Chibante, "Preparation of aqueous latices with *N*-isopropylacrylamide", 247–256, Copyright 1986, with permission from Elsevier. (C) Variation in the mean size of poly(acrylamide) microspheres due to subtle changes in the solvent composition. From Kawaguchi et al., Polymer International, 30, 225–231, 1993.

Figure 11. Materials formed by assembling microspheres produced by precipitation polymerization

(A) Self-assembled and covalently crosslinked monodisperse poly(NIPAAm) microspheres exhibit iridescence. The concentration of the microspheres in solution during crosslinking increases from left to right. From Hu et al., "Hydrogel Opals", *Advanced Materials*, 2001, 13, 1708–1712. Copyright Wiley-VCH Verlag GmbH & Co. KGaA. Reproduced with permission. (B) Poly(NIPAAm-*co*-PEG) microgels crosslinked to a poly(ethylene terephthalate) surface. Reprinted with permission from *Biomacromolecules*, 8, Singh et al., "Covalent Tethering of Functional Microgel Films onto Poly(ethylene terephthalate) Surfaces", 3271–3275. Copyright 2007 American Chemical Society.

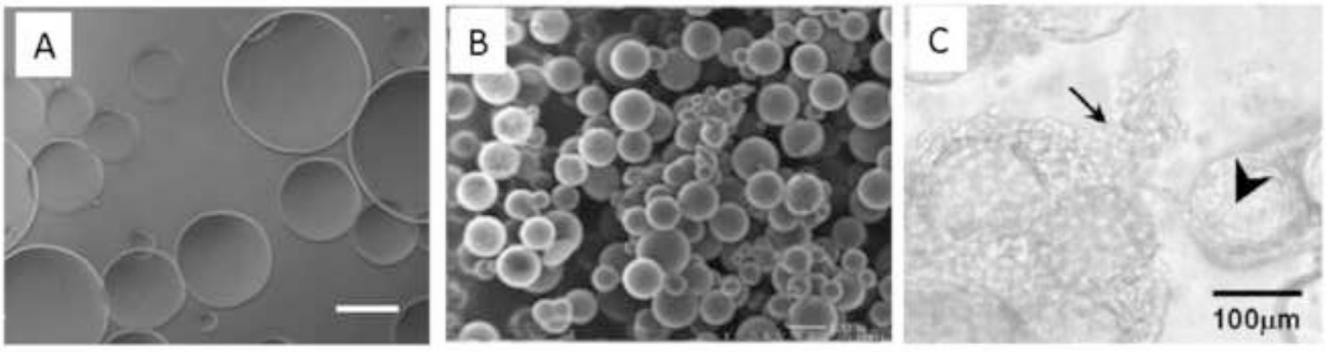

Figure 12. Microspheres formed by inverse (water-in-oil) suspension polymerization

(A) PEG-sebacic acid-diacrylate microspheres free radical crosslinked in water suspended in mineral oil. Scale bar is 200 μm. From Kim et al., *Tissue Engineering C*, 15, 583, 2009. (B) Hyaluronic acid microspheres crosslinked in water suspended in mineral oil. Reprinted from *Biomacromolecules*, 7, Jia et al., "Hyaluronic Acid-Based Microgels and Microgel Networks for Vocal Fold Regeneration", 3336–3344, Copyright 2006, with permission from Elsevier. (C) TGF-β1-loaded gelatin microspheres formed by suspension polymerization in olive oil (large arrow) and chondrocytes (small arrows), both polymerized in an oligo(poly(ethylene glycol)-fumarate) hydrogel. Reprinted from *Biomaterials*, 26, Park et al., "Delivery of TGF-*β*1 and chondrocytes via injectable, biodegradable hydrogels for cartilage tissue engineering applications", 7095–7103, Copyright 2005, with permission from Elsevier.

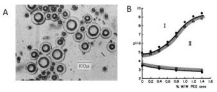

Figure 13. Microspheres formed by aqueous two-phase suspension polymerization

(A) Gelatin/gum arabic complex coacervate surrounding liquid paraffin droplets. (B) Phase diagram for complex coacervate formation between gelatin and gum arabic as a function of pH and PEG concentration. Region I is single phase and Region II is two phase. From Jizomoto, *Journal of Pharmaceutical Sciences* , 74, 469–472, 1985.

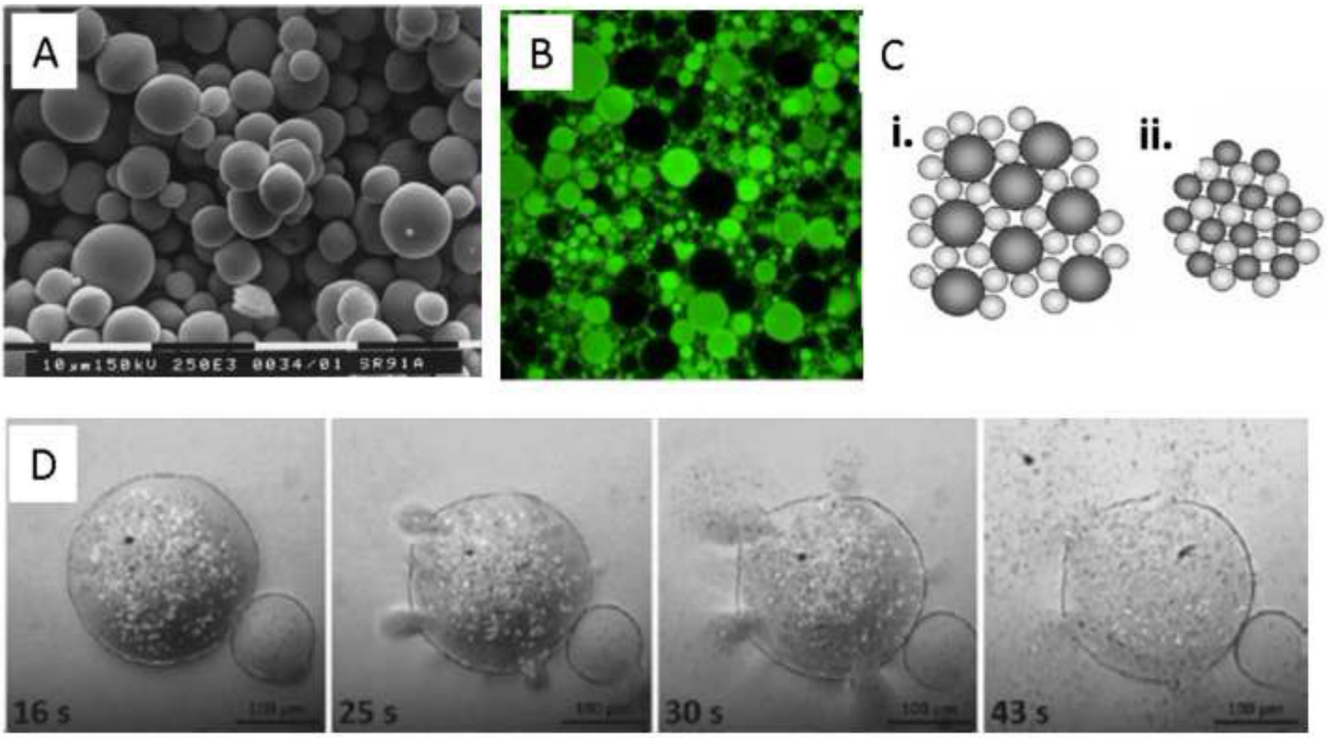

Figure 14. Microspheres formed by aqueous two-phase suspension polymerization

(A) Dextran-methacrylate, PEG and 0.22 M KCl aqueous solutions were mixed and allowed to phase separate. The solution was vigorously mixed for 60 sec then allowed to stabilize for 15 min. Polymerization was initiated by addition of potassium persulfate and TEMED at 37° C. Microspheres were about 10 μm in diameter in the swollen state. Reprinted from *International Journal of Pharmaceutics*, 183, Stenkes et al., "The use of aqueous PEG/dextran phase separation for the preparation of dextran microspheres", 29–32, Copyright 1999 with permission from Elsevier. (B) Dextran-HEMA microspheres were produced as in (A), but without KCl. Charge was introduced by copolymerization with methacrylic acid or dimethylaminoethyl methacrylate. Upon mixing, the oppositely charged microspheres self-assembled to form hydrogels via electrostatic interactions. Fluorescently labeled lysozyme, which is cationic, entered the anionic microspheres but not the cationic microspheres. Reprinted from *Journal of Controlled Release*, 110, Van Tomme et al., "Mobility of model proteins in hydrogels composed of oppositely charged dextran microspheres studied by protein release and fluorescence recovery after photobleaching", 67–78, Copyright 2005, with permission from Elsevier. (C) The strongest self-assembled hydrogels were found when large spheres of one charge were mixed with a larger number of small spheres of opposite charge (i). This presumably led to more efficient packing than with spheres of uniform size (ii). Reprinted from *Biomaterials*, 26, Van Tomme et al., "Self-gelling hydrogels based on oppositely charged dextran microspheres", 2129–2135, Copyright 2005, with permission from Elsevier. (D) Dextran microspheres containing calcium carbonate microparticles were coated with covalently crosslinked polyelectrolyte multilayers. Upon hydrolysis of ester bonds in the dextran microspheres, the higher osmotic pressures led to rapid bursting of the capsules. From De Geest et al., "Self-Exploding Beads Releasing Microcarriers", *Advanced Materials*, 2008, 20, 3687–3691. Copyright Wiley-VCH Verlag GmbH & Co. KGaA. Reproduced with permission.

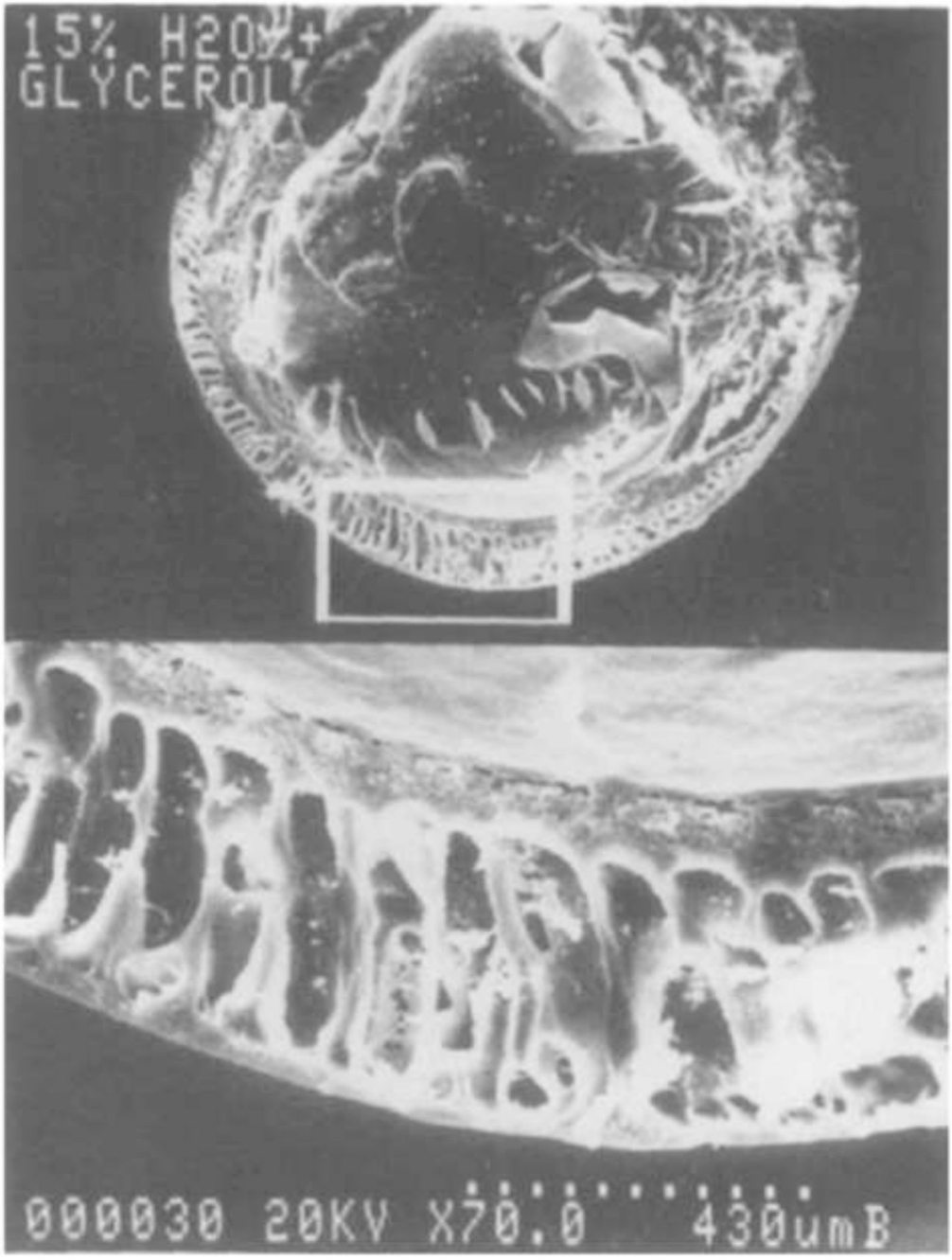

Figure 15. Asymmetric poly(HEMA-*co*-methyl methacrylate) membrane produced by phase inversion

The copolymer dissolved in 85% PEG-200/15% water was flowed coaxially around an aqueous core solution. Droplets were sheared off the tip of a moving needle into an 30% glycerol solution in water. The formed microcapsules were frozen, fractured and visualized by SEM (top). The wall of the capsule (bottom) has a thin homogenous skin and finger-like macrovoids, typical of phase inversion. From Crooks et al., J. Biomed. Mater. Res., 24, 1241–1262, 1990.

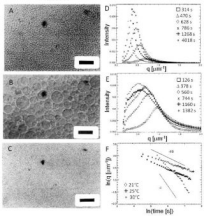

Figure 16. Pinning of phase separation to produce porous materials

(A–C) Gelatin and dextran are soluble in aqueous solutions above 38°C but phase separate below this temperature (UCST behavior, about 38°C). Below 25°C, the gelatin solidifies. (A) Upon rapid cooling from 45°C to 30°C, a phase separation occurred. By 240 seconds, a reticular (net-like) structure was visible. (B) By 1800 seconds, the phases had coarsened to the droplet stage. (C) If the solution was rapidly cooled from 45°C to 21°C, the gelatin solidified, pinning the phase separation at the reticulated stage. (D–F) Light scattering during phase separation showed that the peak intensity moved from higher to lower values of *q* over time, indicating an increase in the characteristic size of the scattering domains. (D) When cooled from 45°C to 30°C, the peak in intensity moved to values of *q* too small to be measured beyond 1268 seconds. (E) When cooled from 45°C to 21°C, the peak intensity became nearly stationary by 744 seconds, indicating that coarsening was pinned. (F) A log-log plot of wave vector maximum versus time showed that coarsening at 30°C occurred with an exponent near 1, and thus the percolation-to-cluster transition was not reached before the wave vector peak became unmeasurable. At 21°C, the growth law exponent was always much smaller than 1, indicating that gelation interfered with coarsening from the earliest stages of phase separation. The growth in size was finally pinned at about 1500 seconds. Reprinted with permission from Tromp et al., *Macromolecules*, 28, 4129–4239, Copyright 1995 American Chemical Society.

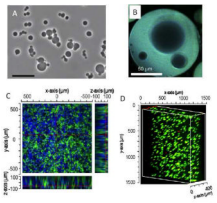

Figure 17. Pinning to produce microspheres

(A) Multiarm PEGs were reacted following a thermally induced phase separation in aqueous sodium sulfate solutions without surfactants or mixing. The time to reach the gel point determined the mean size of the microspheres. Scale bar is 50 μm. (B) Scanning confocal microscopy revealed the presence of solvent-rich pores, likely introduced by ν-induced microsyneresis. (A) & (B) reprinted from *Biomaterials*, 30, Nichols et al., "Factors affecting size and swelling of poly(ethylene glycol) microspheres formed in aqueous sodium sulfate solutions without surfactants", 5283–5291, Copyright 2009 with permission from Elsevier. (C) Using different PEG derivatives as well as albumin, microspheres with specific functionalities were produced and assembled into scaffolds. Structural microspheres are labeled green and drug delivery microspheres are labeled blue. Porogenic microspheres had already dissolved to produce pores in the material. (D) Cell viability was high within the scaffolds. The scaffold was formed in the presence of HepG2 cells, with microspheres crosslinked to each other by reaction with serum proteins. Even following dissolution of the porogenic microspheres, cell viability was greater than 90%. (C) & (D) reprinted from *Acta Biomaterialia*, 6, Scott et al., "Modular scaffolds assembled around living cells using poly(ethylene glycol) microspheres with macroporation via a non-cytotoxic porogen", 29–38, Copyright 2010 with permission from Elsevier.

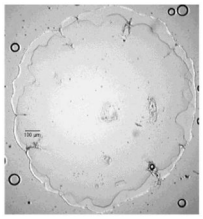

Figure 18. Interfacial polymerization via condensation reactions in a suspension

An aqueous gelatin solution containing living cells was suspended in mineral oil. The amine-crosslinking reagent dithiobis(succinimidylpropionate) was added, which was only soluble in the oil phase. Crosslinking could only occur close to the interface, producing hollow microcapsules. Reprinted from *Biomaterials*, 23, Payne et al., "Development of an injectable, in situ crosslinkable, degradable polymeric carrier for osteogenic cell populations. Part 1. Encapsulation of marrow stromal osteoblasts in surface crosslinked gelatin microparticles", 4359–4371, Copyright 2002 with permission from Elsevier.

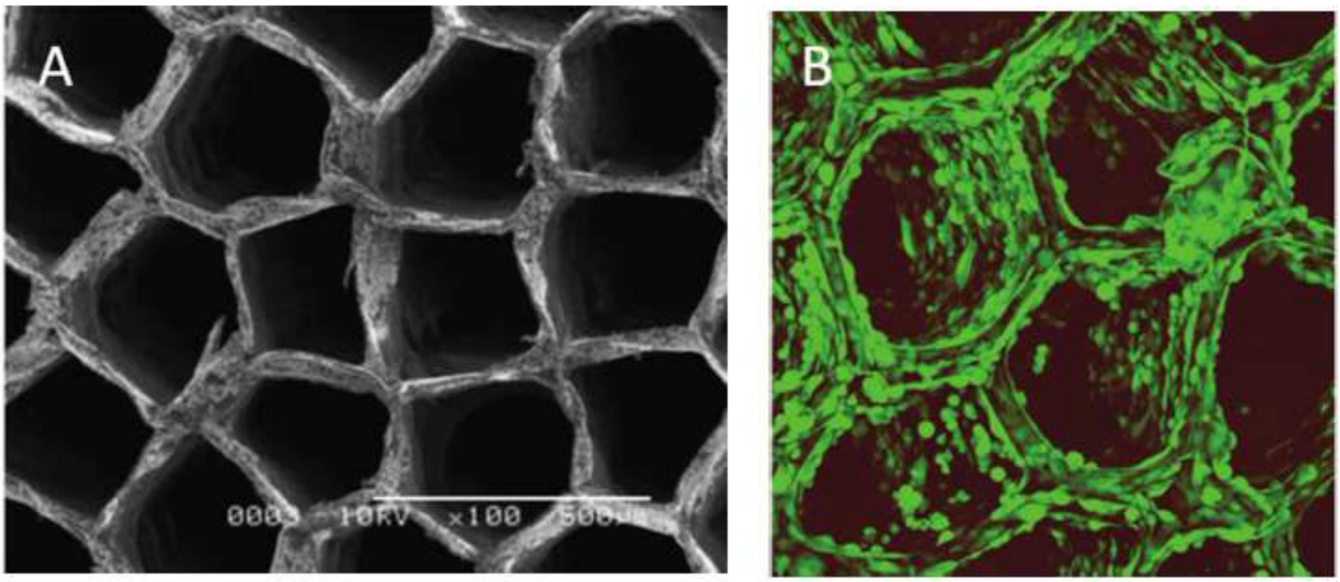

Figure 19. Anisotropic ionotropic gelation

Alginate was crosslinked by only allowing calcium ions to slowly diffuse from the top of the solution to the bottom. Syneresis during crosslinking may have caused lateral contraction of the gel, such that stress was relieved by forming a honeycomb structure. (A) Alginate honeycomb by SEM. (B) Scanning confocal microscopy of GFP labeled cells attached to the honeycomb scaffold. From Yamamoto et al., *Tissue Engineering A*, 16, 299–308, 2010.

Table 1

Different types of heterogeneous polymerizations are distinguished by the solubility of the monomer, initiator and resulting polymer. Rigorous classification also requires study of the kinetics of polymerization.

Polymerization type	**Monomer solubility in continuous phase**	**Initiator solubility in continuous phase**	**Polymer solubility in continuous phase**	**Product**	**Representative Examples**
Suspension	Insoluble	Insoluble	Insoluble	Generally >10 μm particles	153_156,185,187_203
Emulsion	Insoluble	Soluble	Insoluble	Sub-micron particles	225_226
Microsuspension/ Microemulsion/ Miniemulsion	Classification depends on location of initiation *and* kinetics of polymerization (i.e. number of radicals per polymerization locus)				239_243
Precipitation	Soluble	Soluble	Insoluble	Irregular particles, > 1 μm, may produce a porous bulk gel under some conditions	109_114
Dispersion	Soluble	Soluble	Insoluble	Generally 1-10 μm particles	109_114

Table 2

Condensation (step growth) polymerization in two phase systems.

Polymerization type	Monomer A solubility in continuous phase	Monomer B solubility in continuous phase	Polymer solubility in continuous phase	Product	Representative Examples
Suspension	Insoluble	Insoluble, but soluble in same phase as A	Insoluble	Generally >10 μm particles	163_175, 182_184
Emulsion	See Interfacial				
Interfacial	Soluble	Insoluble	Varies	In emulsified systems, may produce microcapsules if polymer insoluble in both phases.	231_235
Precipitation/Dispersion	Soluble	Soluble	Insoluble	Generally 1–10 μm particles	